

Supplementary Information

Indolenine-based derivatives as customizable two-photon fluorescent probes for pH bioimaging in living cells

Carlos Benítez-Martin^{‡,a,c}, Juan A. Guadix^{‡,b,c}, John R. Pearson^c, Francisco Najera^{a,c,*}, Jose M. Perez-Pomares^{b,c,*} and Ezequiel Perez-Inestrosa^{a,c,*}

^a *Universidad de Málaga-IBIMA, Departamento de Química Orgánica. Campus de Teatinos s/n, 29071-Málaga, Spain.*

^b *Departamento de Biología Animal. Facultad de Ciencias. Universidad de Málaga-IBIMA, Campus de Teatinos s/n, 29071 Málaga, Spain.*

^c *Centro Andaluz de Nanomedicina y Biotecnología-BIONAND. Parque Tecnológico de Andalucía, c/Severo Ochoa, 35, 29590 Campanillas, Málaga, Spain.*

[‡] These authors contributed equally to this work.

Corresponding author:

Dr. Francisco Najera

Email: najera@uma.es

Phone: +34 952 13 2023

Postal address: Departamento de Química Orgánica. Facultad de Ciencias. Universidad de Málaga-IBIMA, Campus de Teatinos s/n, 29071 Málaga, Spain.

Prof. Dr. Jose M. Perez-Pomares

Email: jmperezp@uma.es

Phone: +34 952 13 6653

Postal address: Departamento de Biología Animal. Facultad de Ciencias. Universidad de Málaga-IBIMA, Campus de Teatinos s/n, 29071 Málaga, Spain

Prof. Dr. Ezequiel Perez-Inestrosa

Email: inestrosa@uma.es

Phone: +34 952 13 7565

Postal address: Departamento de Química Orgánica. Facultad de Ciencias. Universidad de Málaga-IBIMA, Campus de Teatinos s/n, 29071 Málaga, Spain.

Index

1. EXPERIMENTAL SECTION	4
1.1. GENERAL METHODS AND INSTRUMENTATIONS	4
1.2 SYNTHESIS METHODOLOGIES	4
1.2.1 Synthesis of 1-(6-hydroxynaphthalen-2-yl)-2-methylpropan-1-one (2)	4
1.2.2 Synthesis of 1-(6-(4-bromobutoxy)naphthalen-2-yl)-2-methylpropan-1-one (3a)	4
1.2.3 Synthesis of 1-(6-(2-(2-ethoxyethoxy)ethoxy)naphthalen-2-yl)-2-methylpropan-1-one (3b)	5
1.2.4 Synthesis of 2-(6-(4-bromobutoxy)naphthalen-2-yl)-3,3-dimethyl-3H-indole (4a)	5
1.2.5 Synthesis of 2-(6-(2-(2-ethoxyethoxy)ethoxy)naphthalen-2-yl)-3,3-dimethyl-3H-indole (4b)	6
1.2.6 Synthesis of 2-(6-(4-morpholinobutoxy)naphthalen-2-yl)-3,3-dimethyl-3H-indole (4c)	6
1.3 OPTICAL MEASUREMENTS	7
1.4 TWO-PHOTON MICROSCOPY	7
1.4.1 Cross-section of the protonated compounds 4b+H⁺ and 4c+H⁺	7
1.4.2 Intracellular two-photon microscopy	7
1.5 CELL CULTURE	8
1.6 CELL CYTOTOXICITY ASSAY	8
1.7 CALCULATION METHOD	8
2. ABSORPTION AND EMISSION SPECTRA OF PROBES 4B AND 4C	9
FIGURE S1: ABSORPTION AND EMISSION SPECTRA OF PROBES 4b AND 4c	9
3. OPTICAL RESPONSES TO PH OF COMPOUND 4C AND PKA DETERMINATION	10
FIGURE S2: ABSORPTION AND EMISSION SPECTRA OF COMPOUND 4c AT DIFFERENT PH VALUES	10
4. TD-DFT CALCULATIONS	11
TABLE S1: TD-DFT CALCULATED PHOTOPHYSICAL DATA FOR THE NEUTRAL INDOLENINE AND PROTONATED INDOLIUM SPECIES AT THE PCM(H ₂ O)/CAM-B3LYP/6-31+G(D) LEVEL	11
FIGURE S3: MOLECULAR FRONTIER ORBITALS INVOLVED IN THE S ₁ ←S ₀ TRANSITION FOR THE NEUTRAL INDOLENINE AND PROTONATED IMINIUM AND THE HOMO-LUMO GAP	11
5. NMR TITRATIONS OF PROBE 4B	12
FIGURE S4: ¹ H-NMR TITRATION OF COMPOUND 4b WITH TFA (AROMATIC REGION)	12
6. SELECTIVITY, REVERSIBILITY AND PHOTOSTABILITY OF PROBES 4B AND 4C	13
FIGURE S5: SELECTIVITY STUDIES OF PROBES 4b AND 4c TOWARDS PHYSIOLOGICALLY IMPORTANT METAL IONS	13
FIGURE S6: PH REVERSIBILITY OF PROBES 4b AND 4c BETWEEN PH 7.0 AND 1.2	13
FIGURE S7: PHOTOSTABILITY OF PROBES 4b AND 4c	14
7. TP EXCITATION SPECTRA OF COMPOUNDS 4B AND 4C	15
FIGURE S8: TP EXCITATION SPECTRA OF COMPOUND 4c AND THE PROTONATED 4c+H⁺	15
8. CELL CYTOTOXICITY ASSAY FOR PROBES 4B AND 4C	16
FIGURE S9: CYTOTOXICITY OF COMPOUNDS 4b AND 4c ON MOUSE EMBRYONIC FIBROBLAST (MEF) CELLS	16
9. NEGATIVE CONTROL EXPERIMENTS	17
FIGURE S10: FLUORESCENCE IMAGES OF PROBE NEGATIVE CONTROL MEFs WITHOUT ADDITION OF 4b OR 4c COMPOUNDS AT PH 4.3	17
10. TWO-PHOTON FLUORESCENCE CELL IMAGING	17
FIGURE S11: FLUORESCENCE IMAGES OF PROBE 4b IN MEF CELLS AT DIFFERENT PH VALUES	18
11. CO-LOCALISATION EXPERIMENTS	19
FIGURE S12: MEF CELLS INCUBATED WITH 4c AND LYSOTRACKER DEEP RED	19
12. NMR SPECTRA	20
FIGURE S13: ¹ H-NMR SPECTRUM OF COMPOUND 2 IN CDCl ₃	20
FIGURE S14: ¹³ C-NMR SPECTRUM OF COMPOUND 2 IN CDCl ₃	21
FIGURE S15: ¹ H- ¹ H-COSY SPECTRUM OF COMPOUND 2 IN CDCl ₃	22
FIGURE S16: ¹ H- ¹³ C-HSQC SPECTRUM OF COMPOUND 2 IN CDCl ₃	23
FIGURE S17: ¹ H- ¹³ C-HMBC SPECTRUM OF COMPOUND 2 IN CDCl ₃	24
FIGURE S18: ¹ H-NMR SPECTRUM OF COMPOUND 3a IN CDCl ₃	25
FIGURE S19: ¹³ C-NMR SPECTRUM OF COMPOUND 3a IN CDCl ₃	26
FIGURE S20: ¹ H- ¹ H-COSY SPECTRUM OF COMPOUND 3a IN CDCl ₃	27
FIGURE S21: ¹ H-NMR SPECTRUM OF COMPOUND 3b IN CDCl ₃	28
FIGURE S22: ¹³ C-NMR SPECTRUM OF COMPOUND 3b IN CDCl ₃	29
FIGURE S23: ¹ H- ¹ H-COSY SPECTRUM OF COMPOUND 3b IN CDCl ₃	30
FIGURE S24: ¹ H- ¹³ C-HSQC SPECTRUM OF COMPOUND 3b IN CDCl ₃	31

FIGURE S25: ^1H -NMR SPECTRUM OF COMPOUND 4A IN $\text{DMSO}-D_6$	32
FIGURE S26: ^{13}C -NMR SPECTRUM OF COMPOUND 4A IN $\text{DMSO}-D_6$	33
FIGURE S27: ^1H - ^1H -COSY SPECTRUM OF COMPOUND 4A IN $\text{DMSO}-D_6$	34
FIGURE S28: ^1H - ^{13}C -HSQC SPECTRUM OF COMPOUND 4A IN $\text{DMSO}-D_6$	35
FIGURE S29: ^1H - ^{13}C -HMBC SPECTRUM OF COMPOUND 4A IN $\text{DMSO}-D_6$	36
FIGURE S30: ^1H -NMR SPECTRUM OF COMPOUND 4B IN $\text{DMSO}-D_6$	37
FIGURE S31: ^{13}C -NMR SPECTRUM OF COMPOUND 4B IN $\text{DMSO}-D_6$	38
FIGURE S32: ^1H - ^1H -COSY SPECTRUM OF COMPOUND 4B IN $\text{DMSO}-D_6$	39
FIGURE S33: ^1H - ^{13}C -HSQC SPECTRUM OF COMPOUND 4B IN $\text{DMSO}-D_6$	40
FIGURE S34: ^1H -NMR SPECTRUM OF COMPOUND 4C IN $\text{DMSO}-D_6$	41
FIGURE S35: ^{13}C -NMR SPECTRUM OF COMPOUND 4C IN $\text{DMSO}-D_6$	42
FIGURE S36: ^1H - ^1H -COSY SPECTRUM OF COMPOUND 4C IN $\text{DMSO}-D_6$	43
FIGURE S37: ^1H - ^{13}C -HSQC SPECTRUM OF COMPOUND 4C IN $\text{DMSO}-D_6$	44
13. TWO-PHOTON PH PROBES DESCRIBED IN LITERATURE: BENCHMARK OF THE STATE OF THE ART	45
14. REFERENCES	48

1. Experimental Section

1.1. General methods and instrumentations

Commercially-available reagents and chemicals were used without further purification. Compound **1** was synthesised as described previously.¹ Column chromatography was performed using silica gel 60 (230-400 mesh) and thin layer chromatography (TLC) with silica gel 60 F₂₅₄ plates. ¹H and ¹³C NMR spectra were recorded on a Bruker Advance III Ascend 400 MHz and 101 MHz, respectively. ¹H NMR chemical shifts (δ) are expressed in parts per million (ppm) and are calibrated using residual protic solvent (¹H NMR, CHCl₃ at 7.26 ppm, CHD₅SO at 2.50 ppm). Carbon chemical shifts (δ) are also expressed in parts per million (ppm) and are referenced to the central carbon resonances of the solvents (CDCl₃ at 77.0 ppm or (CD₃)₂SO at 39.5 ppm). In order to assign the ¹H and ¹³C NMR spectra, a range of 2D NMR experiments (COSY, HSQC, HMBC) were used as appropriate. High resolution electrospray ionisation (ESI) mass spectra were obtained on a Thermo Fisher high resolution mass spectrometer Orbitrap and infrared spectra were recorded on a JASCO FT/IR-4100. Melting points were measured in a Gallenkamp melting point apparatus. Absorption spectra were recorded on a Cary 100 Bio UV-Vis Spectrophotometer. Emission and excitation spectra were recorded on a JASCO FP-750 Spectrofluorometer.

1.2 Synthesis methodologies

1.2.1 Synthesis of 1-(6-hydroxynaphthalen-2-yl)-2-methylpropan-1-one (2). Compound **1** (5.0 g, 21.9 mmol) and HBr 48% (25.0 mL, 219.0 mmol) were dissolved in 75 mL of glacial acetic acid in a 250 mL round bottom flask. The mixture was heated to reflux during 24 hours. The reaction was followed by TLC (CH₂Cl₂/*n*-hexane 9:1). Then was concentrated *in vacuo*, dissolved in 100 mL of EtAcO. and washed with 10% NaHCO₃ (2 x 75 mL) and brine (75 mL). The organic layer was dried over anhydrous MgSO₄ and concentrated *in vacuo*. The product was purified by column chromatography using CH₂Cl₂/*n*-hexane (9:1) to CH₂Cl₂ as eluent, obtaining compound **2** as a brown oil (3.25 g, 86% yield). ¹H-NMR (400 MHz, CDCl₃) δ (ppm): 8.42 (d, J = 1.5 Hz, 1H, *H*₁), 7.99 (dd, J = 8.7, 1.5 Hz, 1H, *H*₃), 7.87 (d, J = 8.5 Hz, 1H, *H*₇), 7.71 (d, J = 8.7 Hz, 1H, *H*₄), 7.23–7.17 (m, 2H, *H*₈ and *H*₅), 3.73 (hept, J = 6.9 Hz, 1H, *CH*(CH₃)₂), 1.28 (d, J = 6.9 Hz, 6H, *CH*(CH₃)₂). ¹³C-NMR (101 MHz, CDCl₃) δ (ppm): 205.0 (C=O), 156.0 (C₆), 137.2 (C_{4a}), 131.7 (C₇), 131.4 (C₂), 130.0 (C₁), 127.8 (C_{8a}), 126.9 (C₄), 125.1 (C₃), 118.9 (C₈), 109.6 (C₅), 35.3 (*CH*(CH₃)₂), 19.4 (*CH*(CH₃)₂). IR, ν (cm⁻¹): 3311, 2966, 2918, 2867, 1655, 1616, 1559, 1477, 1280, 1239, 1154, 935, 799, 664. DEP-MS: 214 (M⁺), 171 (M⁺-43), 143 (M⁺-71).

1.2.2 Synthesis of 1-(6-(4-bromobutoxy)naphthalen-2-yl)-2-methylpropan-1-one (3a). Compound **2** (2.60 g, 12.13 mmol) was dissolved in MeOH and KOH (0.88 g, 13.34 mmol) was added. This mixture was heated until reflux for one hour. Then, the resulting alkoxide salt was concentrated *in vacuo*. In a 250 mL two-neck round bottom flask, 1,4-dibromobutane (1.88 mL, 15.77 mmol) was solved in 100 mL of CH₃CN and heated at 80 °C. The alkoxide salt was dispersed in 20 mL of CH₃CN and slowly added to the two-neck round bottom flask through a dropping funnel. After finishing the addition, the temperature was maintained during 2 hours. The reaction was followed by TLC using CH₂Cl₂/*n*-hexane 8:2 as eluent. When the reaction finished, was concentrated *in vacuo* and dissolved in 50 mL of CH₂Cl₂. The solution was washed with 10 % NaHCO₃ (2 x 50 mL) and water (50 mL). The organic layer was dried over anhydrous MgSO₄ and concentrated *in vacuo*. The product was purified by column chromatography using CH₂Cl₂/*n*-hexane (8:2) to afford compound **3a** as a brown oil (3.45 g,

82% yield). ¹H-NMR (400 MHz, CDCl₃) δ (ppm): 8.42 (d, J = 1.7 Hz, 1H, *H*₁), 8.03 (dd, J = 8.7, 1.7 Hz, 1H, *H*₃), 7.88 (d, J = 8.9 Hz, 1H, *H*₈), 7.78 (d, J = 8.7 Hz, 1H, *H*₄), 7.21 (dd, J = 8.9, 2.5 Hz, 1H, *H*₇), 7.17 (d, J = 2.5 Hz, 1H, *H*₅), 4.17 (t, J = 6.5 Hz, 2H, *H*_{1 alk}), 3.73 (hept, J = 6.8 Hz, 1H, *CH(CH*₃*)*₂), 3.55 (t, J = 6.5 Hz, 2H, *H*_{4 alk}), 2.15 (quint, J = 6.5 Hz, 2H, *H*_{2 alk}), 2.06 (quint, J = 6.5 Hz, 2H, *H*_{3 alk}), 1.30 (d, J = 6.8 Hz, 6H, *CH(CH*₃*)*₂). ¹³C-NMR (101 MHz, CDCl₃) δ (ppm): 204.2 (C=O), 158.9 (C₆), 137.1 (C_{4a}), 131.6 (C₇), 131.2 (C₂), 129.6 (C₁), 128.0 (C_{8a}), 127.1 (C₄), 125.1 (C₃), 119.8 (C₈), 106.4 (C₅), 67.0 (C_{1 alk}), 35.2 (*CH(CH*₃*)*₂), 33.4 (C_{4 alk}), 29.5 (C_{2 alk}), 27.8 (C_{3 alk}), 19.4 (*CH(CH*₃*)*₂). IR, ν (cm⁻¹): 3059, 2966, 2931, 2871, 1671, 1620, 1468, 1383, 1261, 1195, 1174, 1016, 989, 855, 811, 743, 648. HRMS (ESI): calculated mass for C₁₈H₂₂O₂Br₁ (M+H⁺): 349.0798; found 349.0799.

1.2.3 Synthesis of 1-(6-(2-(2-ethoxyethoxy)ethoxy)naphthalen-2-yl)-2-methylpropan-1-one (3b). Compound **2** (0.65 g, 3.03 mmol) and 2-(2-ethoxyethoxy)ethyl 4-methylbenzenesulfonate (0.67 g, 2.33 mmol) were dissolved in 5 mL of DMF in a 25 mL round bottom flask and K₂CO₃ (0.84 g, 6.06 mmol) was added to the mixture. The mixture was heated to 80°C overnight. The reaction was followed by TLC using CH₂Cl₂/EtAcO (95:5) as eluent. Then, 50 mL of EtAcO were added and washed with saturated NaHCO₃ (2 x 15 mL) and 10% Na₂CO₃ (15 mL). The organic layer was dried over anhydrous MgSO₄ and concentrated *in vacuo*. The syrup obtained was purified by column chromatography using CH₂Cl₂/EtAcO (95:5) as eluent, obtaining compound **3b** as a brown oil (0.70 g, 91% yield). ¹H-NMR (400 MHz, CDCl₃) δ (ppm): 8.32 (d, J = 1.8 Hz, 1H, *H*₁), 7.92 (dd, J = 8.6, 1.8 Hz, 1H, *H*₃), 7.77 (d, J = 9.0 Hz, 1H, *H*₈), 7.68 (d, J = 8.6 Hz, 1H, *H*₄), 7.16 (dd, J = 9.0, 2.5 Hz, 1H, *H*₇), 7.08 (d, J = 2.5 Hz, 1H, *H*₅), 4.21 (t, J = 4.8 Hz, 2H, *H*_{1 alk}), 3.87 (d, J = 4.8 Hz, 2H, *H*_{2 alk}), 3.68 (d, J = 5.0 Hz, 2H, *H*_{3 alk}), 3.62 (hept, J = 6.8 Hz, 1H, *CH(CH*₃*)*₂), 3.56 (t, J = 5.0 Hz, 2H, *H*_{4 alk}), 3.47 (q, J = 6.9 Hz, 2H, *H*_{5 alk}), 1.19 (d, J = 6.9 Hz, 6H, *CH(CH*₃*)*₂), 1.14 (t, J = 7.0 Hz, 3H, *H*_{6 alk}). ¹³C-NMR (101 MHz, CDCl₃) δ (ppm): 204.2 (C=O), 158.8 (C₆), 137.1 (C_{4a}), 131.6 (C₂), 131.1 (C₈), 129.6 (C₁), 128.0 (C_{8a}), 127.2 (C₄), 125.1 (C₃), 119.9 (C₇), 106.6 (C₅), 71.0 (C_{3 alk}), 69.9 (C_{4 alk}), 69.6 (C_{2 alk}), 67.6 (C_{1 alk}), 66.7 (C_{5 alk}), 35.2 (*CH(CH*₃*)*₂), 19.4 (*CH(CH*₃*)*₂), 15.2 (C_{6 alk}). IR, ν (cm⁻¹): 3061, 2968, 2928, 2871, 2359, 1672, 1621, 1470, 1383, 1349, 1262, 1196, 1151, 990, 856, 813, 743. HRMS (ESI): calculated mass for C₂₀H₂₇O₄ (M+H⁺): 331.1904; found, 331.1903.

1.2.4 Synthesis of 2-(6-(4-bromobutoxy)naphthalen-2-yl)-3,3-dimethyl-3H-indole (4a). Compound **3a** (3.40 g, 9.74 mmol) and phenylhydrazine hydrochloride (1.41 g, 9.74 mmol) were dissolved in 20 mL of glacial AcOH in a 50 mL round bottom flask. The mixture was heated to reflux for 24 hours. The reaction was followed by TLC using CH₂Cl₂ as eluent. The reaction was then concentrated *in vacuo*, redissolved in 50 mL of CH₂Cl₂ and washed with saturated Na₂CO₃ (2 x 30 mL) and brine (2 x 30 mL). Finally, the organic layer was dried over anhydrous MgSO₄ and concentrated *in vacuo*. The product was purified by column chromatography using CH₂Cl₂ as eluent, obtaining the compound **4a** as a yellow solid (3.34 g, 81% yield). M.p.: 132-133 °C. ¹H-NMR (400 MHz, DMSO-*d*₆) δ (ppm): 8.60 (d, J = 1.8 Hz, 1H, *H*_{1 naph}), 8.35 (dd, J = 8.7, 1.8 Hz, 1H, *H*_{3 naph}), 8.12 (d, J = 9.0 Hz, 1H, *H*_{8 naph}), 7.90 (d, J = 8.7 Hz, 1H, *H*_{4 naph}), 7.63 (d, J = 7.5 Hz, 1H, *H*₄), 7.55 (d, J = 7.1 Hz, 1H, *H*₇), 7.40 (d, J = 2.5 Hz, 1H, *H*_{5 naph}), 7.37 (td, J = 7.5, 1.2 Hz, 1H, *H*₅), 7.29 (td, J = 7.1, 0.8 Hz, 1H, *H*₆), 7.25 (dd, J = 9.0, 2.5 Hz, 1H, *H*_{7 naph}), 4.20 (t, J = 6.1 Hz, 2H, *H*_{1 alk}), 3.76 (d, J = 6.3 Hz, 1H, *H*_{4 alk}), 3.65 (t, J = 6.6 Hz, 1H, *H*_{4 alk}), 2.08–1.88 (m, 4H, *H*_{2 alk} and *H*_{3 alk}), 1.64 (s, 6H, C(CH₃)₂). ¹³C-NMR (101 MHz, DMSO-*d*₆) δ (ppm): 182.8 (C₂), 158.4 (C_{6 naph}), 153.2 (C_{3a}), 148.5 (C_{7a}), 135.9 (C_{4a naph}), 131.4 (C_{8 naph}), 128.8 (C_{1 naph}), 128.5 (C_{2 naph}), 128.1 (C_{8a naph} and C₅), 127.5 (C_{4 naph}), 126.2 (C_{3 naph}), 126.1 (C₆), 121.9 (C₇), 120.7 (C₄), 119.6 (C_{7 naph}), 107.3 (C_{5 naph}), 67.4 (C_{1 alk}), 67.3 (C_{1 alk}), 53.4 (C(CH₃)₂), 45.7 (C_{4 alk}), 35.3

($C_{4\text{ alk}}$), 29.6, 29.4, 27.8 and 26.6 ($C_{2\text{ alk}}$ and $C_{3\text{ alk}}$), 25.0 ($C(\underline{CH_3})_2$). IR, ν (cm^{-1}): 3059, 2950, 2927, 2871, 1627, 1609, 1522, 1472, 1455, 1393, 1205, 1173, 1019, 887, 865, 810, 773, 756, 650. HRMS (ESI): calculated mass for $C_{24}H_{25}N_1O_1Br_1$ ($M+H^+$): 422.1114; found, 422.1112.

1.2.5 Synthesis of 2-(6-(2-(2-ethoxyethoxy)ethoxy)naphthalen-2-yl)-3,3-dimethyl-3H-indole (4b). Compound **3b** (0.77 g, 2.33 mmol) and phenylhydrazine hydrochloride (0.34 g, 2.33 mmol) were dissolved in 10 mL of glacial AcOH in a 25 mL round bottom flask. The mixture was heated to reflux for 24 hours. The reaction was followed by TLC using CH_2Cl_2 /EtAcO (95:5) as eluent. The reaction was concentrated *in vacuo*, dissolved in 25 mL of CH_2Cl_2 and washed with Na_2CO_3 conc. (2 x 15 mL) and brine (2 x 15 mL). Finally, the organic layer was dried over anhydrous $MgSO_4$ and concentrated *in vacuo*. The product was purified by column chromatography using CH_2Cl_2 /EtAcO (95:5) as eluent, obtaining compound **4b** as a brownish oil (0.69 g, 74% yield). 1H -NMR (400 MHz, $DMSO-d_6$) δ (ppm): 8.62 (d, $J=1.7$ Hz, 1H, $H_{1\text{ naph}}$), 8.36 (dd, $J=8.8, 1.7$ Hz, 1H, $H_{3\text{ naph}}$), 8.14 (d, $J=8.9$ Hz, 1H, $H_{8\text{ naph}}$), 7.90 (d, $J=8.8$ Hz, 1H, $H_{4\text{ naph}}$), 7.63 (d, $J=7.5$ Hz, 1H, H_4), 7.56 (d, $J=6.9$ Hz, 1H, H_7), 7.41 (d, $J=2.4$ Hz, 1H, $H_{5\text{ naph}}$), 7.37 (td, $J=7.5, 1.2$ Hz, 1H, H_5), 7.29 (td, $J=6.9, 0.8$ Hz, 1H, H_6), 7.26 (dd, $J=8.9, 2.4$ Hz, 1H, $H_{7\text{ naph}}$), 4.27 (t, $J=4.8$ Hz, 2H, $H_{1\text{ alk}}$), 3.84 (t, $J=4.8$ Hz, 2H, $H_{2\text{ alk}}$), 3.63 (t, $J=5.8$ Hz, 2H, $H_{3\text{ alk}}$), 3.52 (t, $J=5.8$ Hz, 2H, $H_{4\text{ alk}}$), 3.45 (q, $J=7.0$ Hz, 2H, $H_{5\text{ alk}}$), 1.64 (s, 6H, $C(\underline{CH_3})_2$), 1.11 (t, $J=7.0$ Hz, 3H, $H_{6\text{ alk}}$). ^{13}C -NMR (101 MHz, $DMSO-d_6$) δ (ppm): 182.8 (C_2), 158.3 ($C_{6\text{ naph}}$), 153.2 (C_{3a}), 148.5 (C_{7a}), 135.9 ($C_{4a\text{ naph}}$), 131.4 ($C_{8\text{ naph}}$), 128.8 ($C_{1\text{ naph}}$), 128.5 ($C_{2\text{ naph}}$), 128.1 ($C_{8a\text{ naph}}$), 128.1 (C_5), 127.6 ($C_{4\text{ naph}}$), 126.2 ($C_{3\text{ naph}}$), 126.2 (C_6), 121.9 (C_7), 120.7 (C_4), 119.6 ($C_{7\text{ naph}}$), 107.3 ($C_{5\text{ naph}}$), 70.5 ($C_{3\text{ alk}}$), 69.7 ($C_{4\text{ alk}}$), 69.3 ($C_{2\text{ alk}}$), 67.8 ($C_{1\text{ alk}}$), 66.1 ($C_{5\text{ alk}}$), 53.4 ($C(\underline{CH_3})_2$), 25.0 ($C(\underline{CH_3})_2$), 15.6 ($C_{6\text{ alk}}$). IR, ν (cm^{-1}): 3060, 2969, 2925, 2866, 1625, 1602, 1519, 1453, 1272, 1255, 1206, 1107, 752. HRMS (ESI): calculated mass for $C_{26}H_{30}N_1O_3$ ($M+H^+$): 404.2220; found, 404.2219.

1.2.6 Synthesis of 2-(6-(4-morpholinobutoxy)naphthalen-2-yl)-3,3-dimethyl-3H-indole (4c). Compound **4a** (0.30 g, 0.71 mmol), KI (0.03 g, 0.18 mmol) and K_2CO_3 (0.10 g, 0.75 mmol) were added to a 25 mL round bottom flask, then DMF (5 mL) and morpholine (0.20 mL, 2.24 mmol). The mixture was heated to 80 °C overnight. The reaction was followed by TCL using CH_2Cl_2 /MeOH (95:5) as eluent. When the reaction was finished, 40 mL of CH_2Cl_2 were added and washed with HCl 2M (2 x 40 mL). The aqueous layer was neutralised with NaOH 2M (90 mL). Then, the aqueous layer was extracted with CH_2Cl_2 (2 x 50 mL). Finally, the organic layer was dried over anhydrous $MgSO_4$ and concentrated *in vacuo* obtaining compound **4c** as a yellow solid (0.26 g, 86% yield). M.p.: 104-105 °C. 1H -NMR (400 MHz, $DMSO-d_6$) δ (ppm): 8.61 (d, $J=1.7$ Hz, 1H, $H_{1\text{ naph}}$), 8.35 (dd, $J=8.7, 1.7$ Hz, 1H, $H_{3\text{ naph}}$), 8.12 (d, $J=9.0$ Hz, 1H, $H_{8\text{ naph}}$), 7.90 (d, $J=8.7$ Hz, 1H, $H_{4\text{ naph}}$), 7.63 (d, $J=7.5$ Hz, 1H, H_4), 7.56 (d, $J=7.1$ Hz, 1H, H_7), 7.39 (d, $J=2.3$ Hz, 1H, $H_{5\text{ naph}}$), 7.37 (td, $J=7.5, 1.2$ Hz, 1H, H_5), 7.29 (td, $J=7.1, 0.8$ Hz, 1H, H_6), 7.24 (dd, $J=9.0, 2.3$ Hz, 1H, $H_{7\text{ naph}}$), 4.16 (t, $J=6.5$ Hz, 2H, $H_{1\text{ alk}}$), 3.57 (t, $J=4.6$ Hz, 4H, $O-(CH_2)_2\text{ morph}$), 2.36 (t, $J=7.1$ Hz, 6H $N-(CH_2)_2\text{ morph}$ and $H_{4\text{ alk}}$), 1.83 (quint, $J=6.5$ Hz, 2H, $H_{2\text{ alk}}$), 1.68–1.59 (m, 8H, $C(\underline{CH_3})_2$ and $H_{3\text{ alk}}$). ^{13}C -NMR (101 MHz, $DMSO-d_6$) δ (ppm): 182.8 (C_2), 158.5 ($C_{6\text{ naph}}$), 153.2 (C_{3a}), 148.5 (C_{7a}), 135.9 ($C_{4a\text{ naph}}$), 131.4 ($C_{8\text{ naph}}$), 128.8 ($C_{1\text{ naph}}$), 128.4 ($C_{2\text{ naph}}$), 128.1 ($C_{8a\text{ naph}}$), 128.0 (C_5), 127.5 ($C_{4\text{ naph}}$), 126.2 ($C_{3\text{ naph}}$), 121.9 (C_7), 120.6 (C_4), 119.7 ($C_{7\text{ naph}}$), 107.2 ($C_{5\text{ naph}}$), 68.0 ($C_{1\text{ alk}}$), 66.7 ($O-(CH_2)_2\text{ morph}$), 58.3 ($C(\underline{CH_3})_2$), 53.8 and 53.4 ($N-(CH_2)_2\text{ morph}$ and $C_{4\text{ alk}}$), 27.0 ($C_{2\text{ alk}}$), 25.0 ($C(\underline{CH_3})_2$), 22.9 ($C_{3\text{ alk}}$). IR, ν (cm^{-1}): 3061, 2928, 2847, 2800, 2763, 1626, 1608, 1519, 1454, 1273, 1256, 1116, 979, 867, 813, 751, 652. HRMS (ESI): calculated mass for $C_{24}H_{25}N_1O_1Br_1$ ($M+H^+$): 422.1114; found, 422.1112.

1.3 Optical measurements

All absorption and emission spectra were recorded using 10 μ M solutions from stock solutions 1.0 mM DMSO of compounds **4b** and **4c** in 1 cm path length quartz fluorescence cuvette at room temperature. The slit widths of excitation and emission were set to 5 nm in both cases. Fluorescence quantum yields were determined using Coumarine 153 in EtOH ($\Phi_F=0.380$) or quinine sulphate in H₂SO₄ 0.5M ($\Phi_F=0.546$) following the IUPAC standard methodology.²

For the pH titration, Absorption and emission spectra were recorded at different pH water solutions (1% DMSO), modifying pH by addition of HCl and NaOH (1M in both cases) and registering pH with a well-calibrated pH-meter. Therefore, pK_a was determined from data recorded for both compounds, using the Henderson-Hasselbach-type mass action equation: $pH = \log[(I_{max} - I)/(I - I_{min})] + pK_a$. In this equation, I_{max} and I_{min} are the highest and lowest values of absorbance or fluorescence intensity obtained in the pH range studied. I is the absorbance or intensity for the considered pH. The origin coordinate is the pK_a value.

The selectivity was studied through various aqueous solutions of the different compounds (10 μ M) that contained each different metallic ion at different pH values (1.22 and 7.00).

The reversibility was investigated modifying pH repeatedly between 1.22 and 7.00 using concentrated hydrochloric acid and aqueous ammonia in a 10 μ M aqueous solution of the different derivatives.

Photostability studies were carried out at 10 μ M compound concentrations. These studies were first performed in neutral water and then in a pH-adjusted hydrochloric acid buffer (pH=1.22).

1.4 Two-photon microscopy

1.4.1 Cross-section of the protonated compounds **4b+H⁺ and **4c+H⁺**.** The two-photon absorption cross-sections (σ) were determined according to a standard procedure,³ and within a laser power regime where the fluorescence is proportional to the square of the laser excitation power by two-photon-excitation fluorescence measurements. Rhodamine B (10⁻⁵ M in MeOH) was used as a reference, assuming that the fluorescence quantum yield is the same regardless of whether two- or one- photon excitation is used. The fluorescence properties of the compound were analysed using an inverted Leica SP5 MP confocal microscope equipped with a MaiTai Ti:Sapphire HP laser (Spectra-Physics, Inc.) tuneable between 690 and 1040 nm. Imaging was performed using a 10x Plan APO objective (NA 0.4) focused at the air/liquid boundary, allowing the simultaneous detection of sample and background fluorescence. Emission and excitation spectra data for compound and background regions of interest (ROIs) were registered using Leica LAS AF software. Emission spectra were measured using a dynamic 30 nm wide emission detection window moving in 20 steps between 380 and 700 nm.

1.4.2 Intracellular two-photon microscopy. Intracellular fluorescence and distribution of the two-photon fluorescent probes in cells were analysed using an inverted Leica SP5 MP and a 63x PLAN APO NA 1.4 oil immersion objective. Optimal conditions were maintained throughout the imaging process with an integrated microscope enclosure keeping cells at 37°C and 5% CO₂. These compounds were visualised with two-photon excitation at 800 nm and fluorescence detection between 500-550 nm using a HyD non-descanned detector. Brightfield images were captured independently using a 405 nm laser as light source. Details about co-localisation experiments can be found in section 10.

1.5 Cell culture

MEF cells were isolated from 14.5 old mouse embryos following standard protocols,⁴ and were cultured in complete medium (DMEM + 10% FBS + 1% Penicillin-Streptomycin + 2 mM L-Glutamine) at 37°C in a humidified environment with 5% CO₂. For microscopy experiments, MEF cells were grown in 35 mm glass-bottomed dishes (Ibidi) suitable for optical microscopy to approximately 50% confluency prior to starting the experiment.

In order to study intracellular pH fluctuations in living cells, MEF cells were treated with **4b** or **4c** in PBS pH 7.6 for one hour. To equilibrate the intracellular pH with external pH, cells were incubated in citric acid/phosphate buffer adjusted to various pHs (7.60, 4.30 and 3.30). These buffers were supplemented with 10 nM nigericin (a well-known K⁺/H⁺ ionophore) and 140 mM KCl.⁵

1.6 Cell cytotoxicity assay

A standard cell proliferation reagent, WST-1, was used to test the cytotoxicity of compounds **4b** and **4c** in MEF cells. These were cultured in a 96-well microplate to a total volume of 100 µL per well with a density of 6×10^5 cells per mL at 37 °C in a 5% CO₂ atmosphere. After 24 h, these compounds were incubated at 0.01 µM, 0.025 µM, 0.05 µM, 0.1 µM, 0.5 µM, 1.0 µM, 2.5 µM, 5.0 µM and 10.0 µM concentrations with MEF cells in fresh medium. Cells cultured without any compound were used as negative controls. After incubating the cells for 12 h, 10 µL of WST-1 reagent was added into each of the 96-well microplate for another 6 h. Finally, well absorbance was measured at 440 nm and cell viability calculated using the equation: % viability = $[\sum(A_i/A_{\text{control}} \times 100)]/n$, where A_i is the experimental absorbance value and A_{control} is the average absorbance of the control wells. Three replicas were performed for each sample (n=3).

1.7 Calculation method

Theoretical calculations were performed with the Gaussian 09 program package.⁶ The polarizable continuum model (PCM),⁷ was used to consider the solvent effect and water as solvent. We have substituted the alkoxy chains in compounds **4b** and **4c** by a methoxy group, as it is predictable that the length of these have no considerable influence on their optical properties. The ground-state (S_0) and the excited state (S_1) geometrical parameters were determined by density-functional theory (DFT) using the CAM-B3LYP⁸ functional and the 6-31+G(d) basis set. In each optimisation, the vibrational frequencies were calculated and the results showed that optimised structures were stable geometric ones. Energy parameters were calculated as vertical electronic excitations from the minima of the S_0 or S_1 structures using the linear response (LR) approach and the time-dependent density functional response theory (TD-DFT) employing the same level of theory for the first ten excited states.

2. Absorption and emission spectra of probes 4b and 4c.

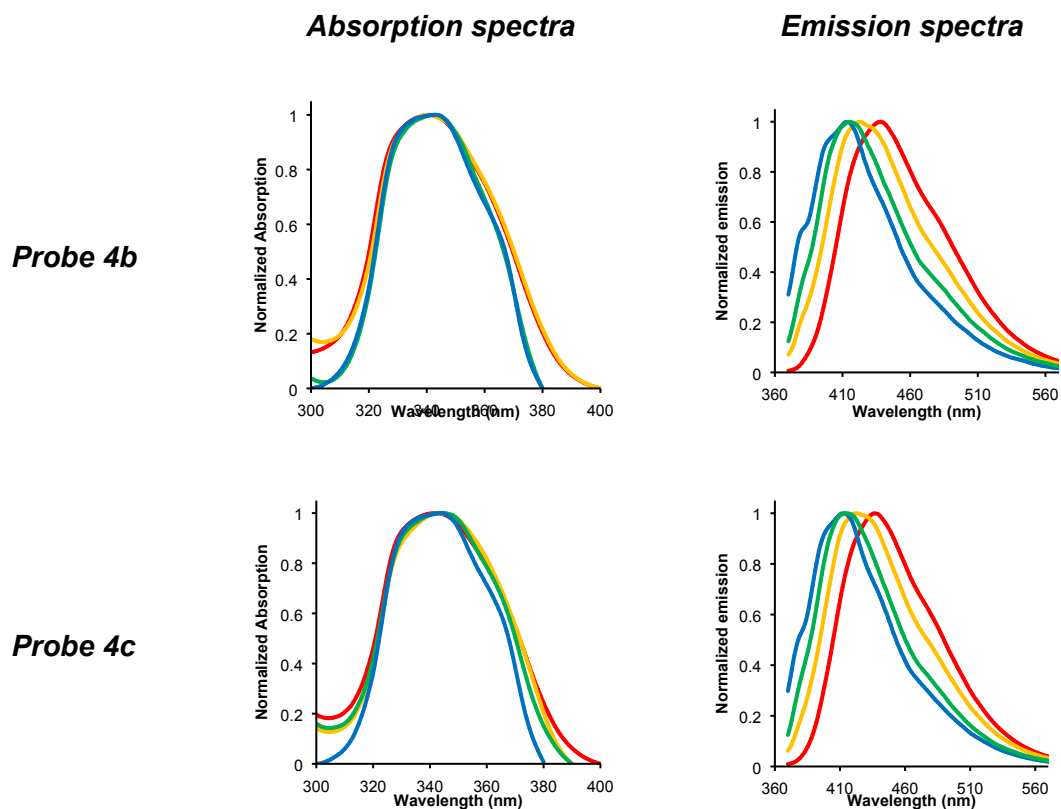


Figure S1: Absorption and emission spectra of probes **4b** and **4c**. Solvents: tetrahydrofuran (blue), dichloromethane (green), methanol (orange), water (red). All measurements were done at 10 μ M concentrations in air equilibrated solutions.

3. Optical responses to pH of compound 4c and pKa determination.

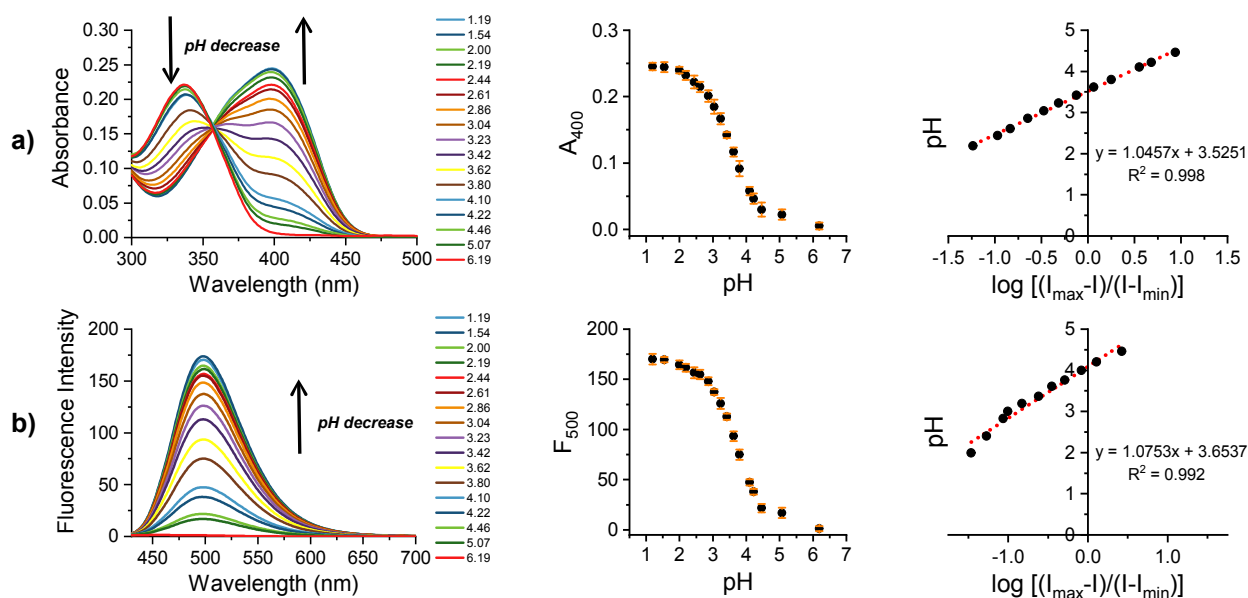


Figure S2: Absorption (row a) and emission (row b) spectra of compound **4c** at different pH values. Plot of absorbance (at 400 nm, row a) and emission (at 500 nm, row b) *versus* pH value (mean of three independent experiments). Representation of the Henderson-Hasselbach mass equation for the absorbance (row a) and emission (row b) data. The pH was modified from 1.19 to 6.19.

4. TD-DFT calculations.

Table S1: TD-DFT calculated photophysical data for the neutral indolenine and protonated indolium species at the PCM(H₂O)/CAM-B3LYP/6-31+G(d) level.

	Transition (<i>f</i>)	E_{calc}^a eV (nm)	E_{exp} eV (nm)	Dominant Components ^b (%)	HOMO-LUMO gap eV
Absorption					
neutral	$S_1 \leftarrow S_0$ (1.108)	3.70 (335.09)	3.74 (332)	LUMO \leftarrow HOMO (94)	6.22
protonated	$S_1 \leftarrow S_0$ (1.133)	3.14 (394.85)	3.10 (400)	LUMO \leftarrow HOMO (95)	5.57
Emission					
neutral	$S_1 \rightarrow S_0$ (1.211)	2.77 (447.60)	3.02 (410)	LUMO \rightarrow HOMO (97)	
protonated	$S_1 \rightarrow S_0$ (1.223)	2.62 (473.22)	2.47 (502)	LUMO \rightarrow HOMO (97)	

^a Obtained using the linear response (LR) approach. ^b Components with greater than 10% contribution shown.

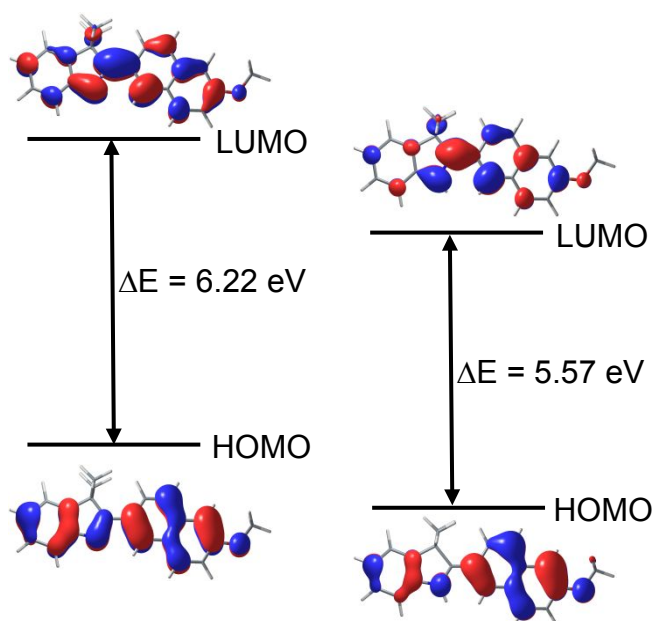


Figure S3: Molecular frontier orbitals (0.03 e/bohr³ isodensity surface) involved in the $S_1 \leftarrow S_0$ transition for the neutral indolenine (left) and protonated iminium (right) and the HOMO-LUMO gap for the neutral (left) and its protonated form (right).

5. NMR titrations of probe 4b.

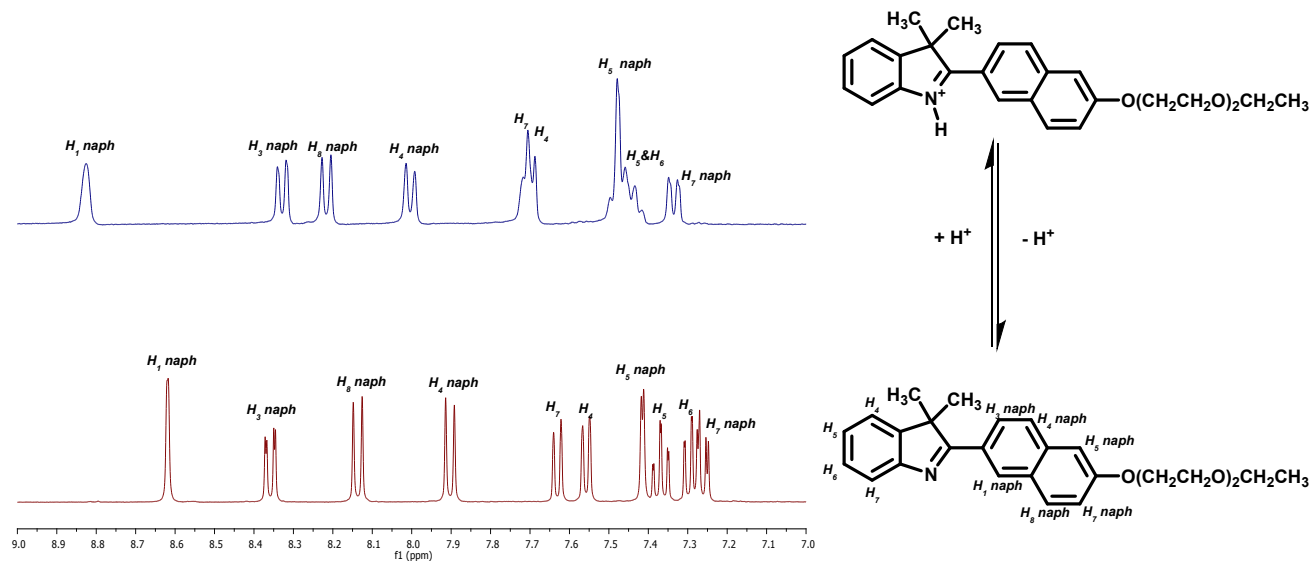


Figure S4: ^1H -NMR titration of compound **4b** with TFA (aromatic region).

6. Selectivity, reversibility and photostability of probes 4b and 4c.

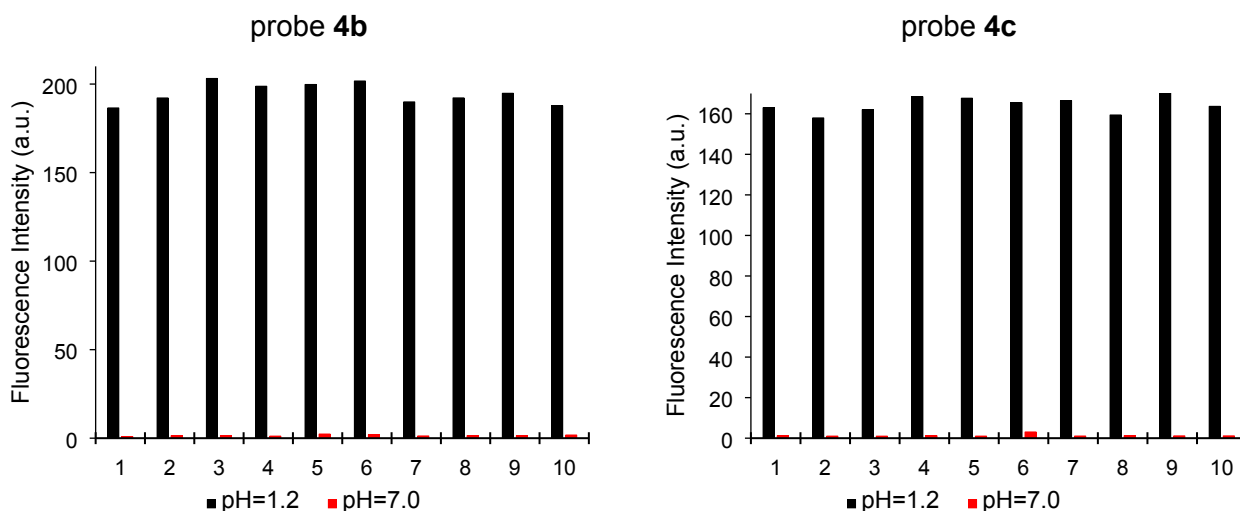


Figure S5: selectivity studies of probes **4b** and **4c** towards physiologically important metal ions (1: Control, 2: Na⁺, 3: Mg²⁺, 4: K⁺, 5: Ca²⁺, 6: Fe²⁺, 7: Cu²⁺, 8: Zn²⁺, 9: Ni²⁺, 10: Co²⁺). 10 μ M solutions of the compounds and the corresponding ions were prepared in pure water (pH = 7.00) and aqueous HCl solution (pH = 1.22) with 1% DMSO. Emission at 500 nm was recorded after exciting at 400 nm in all cases.

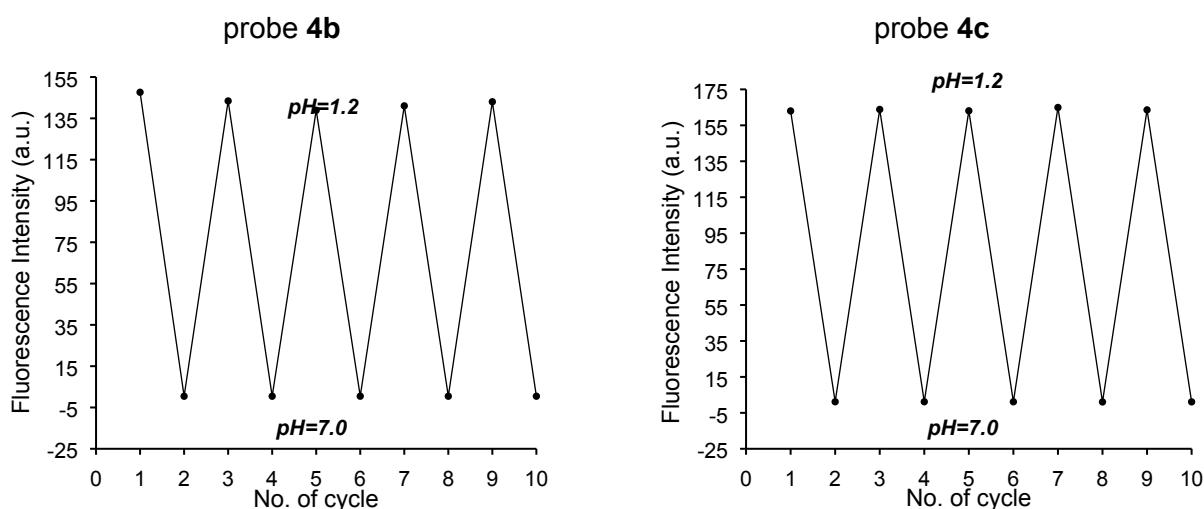


Figure S6: pH reversibility of probes **4b** and **4c** between pH 7.00 and 1.22. Aqueous solutions 10 μ M (1% DMSO) were employed. Emission at 500 nm was recorded after exciting at 400 nm in all cases.

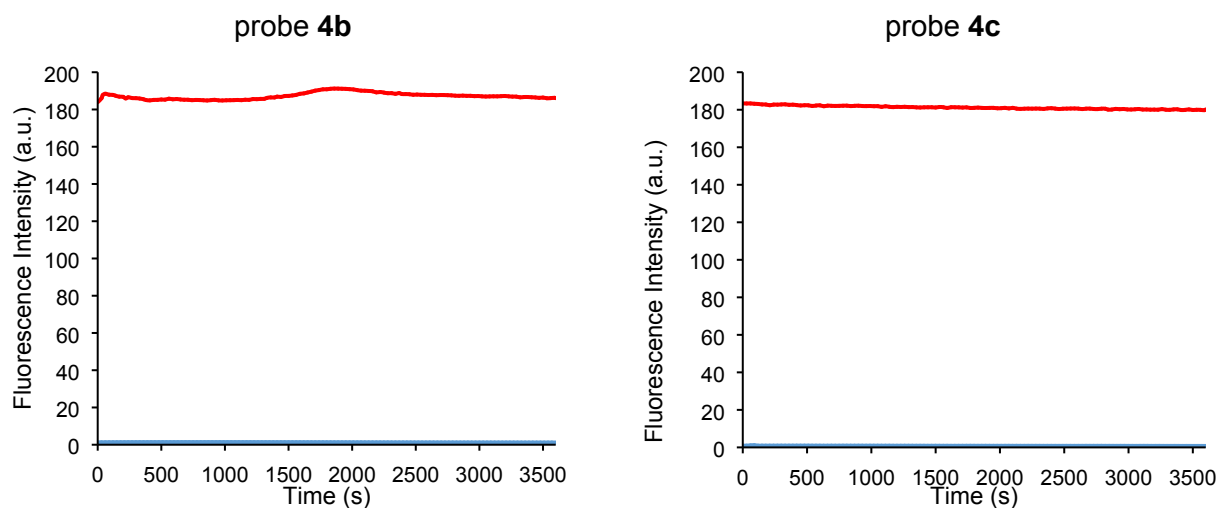


Figure S7: Photostability of probes **4b** and **4c**. Solutions 10 μ M of compounds were prepared in pure water (pH = 7.0) (blue) and aqueous HCl solution (pH = 1.22) (red) with 1% DMSO. Emission at 500 nm was recorded after exciting at 400 nm in all cases.

7. TP Excitation spectra of compounds 4b and 4c.

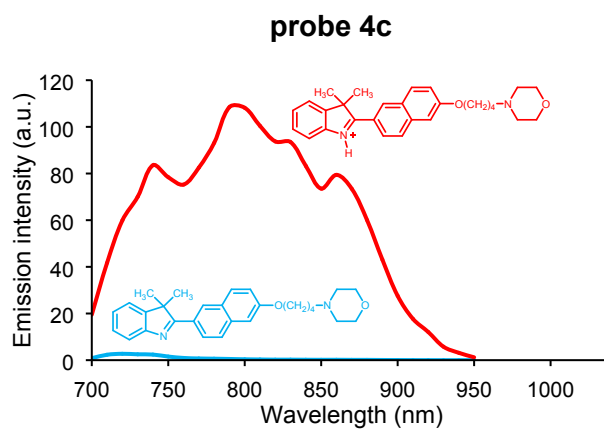


Figure S8: TP Excitation spectra of compound **4c** (blue) and the protonated **4c+H⁺** (red).

8. Cell cytotoxicity assay for probes 4b and 4c.

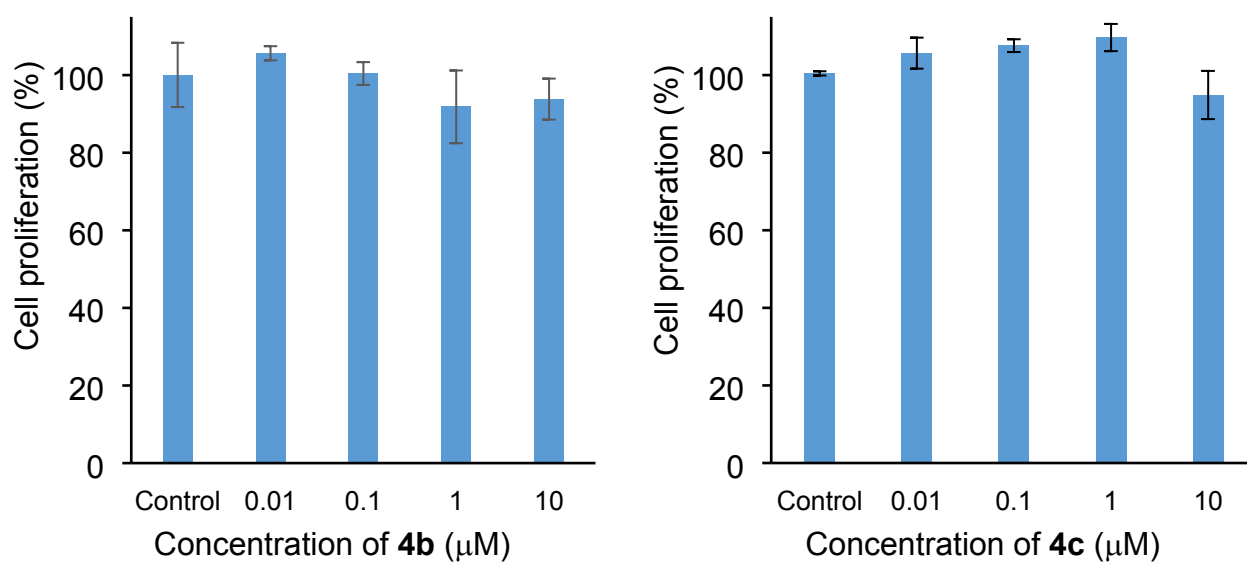


Figure S9: Cytotoxicity of compounds **4b** and **4c** on mouse embryonic fibroblast (MEF) cells. Data are the mean values from independent experiments (n=3).

9. Negative Control Experiments.

MEF cells were isolated from 14.5 old mouse embryos and were cultured in complete medium (DMEM + 10% FBS + 1% Penicillin-Streptomycin + 2 mM L-Glutamine) at 37°C in a humidified environment with 5% CO₂. For microscopy experiments, MEF cells were grown in 35 mm glass-bottomed dishes (Ibidi) suitable for optical microscopy to approximately 50% confluency prior to starting the experiment. MEF cells were treated with PBS pH 7.6 for one hour. To equilibrate the intracellular pH with external pH, cells were incubated in citric acid/phosphate buffer adjusted to various pHs (7.60, 4.35 and 3.30). These buffers were supplemented with 10 nM nigericin and 140 mM KCl.

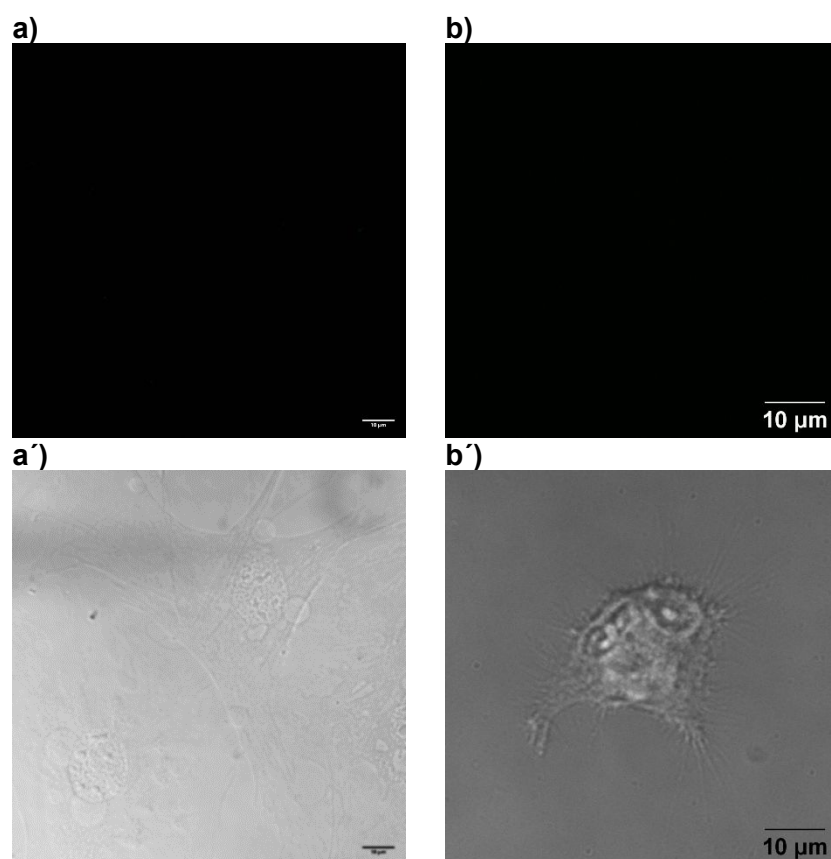


Figure S10: (a-b) Fluorescence images of probe negative control MEFs without addition of **4b** or **4c** compounds at pH 4.3 (10^{-5} M, TP excitation: $\lambda_{\text{exc}} = 800$ nm, $\lambda_{\text{em}} = 500 - 550$ nm) and (a'-b') brightfield in MEF cells at pH 4.3.

10. Two-photon fluorescence cell imaging.

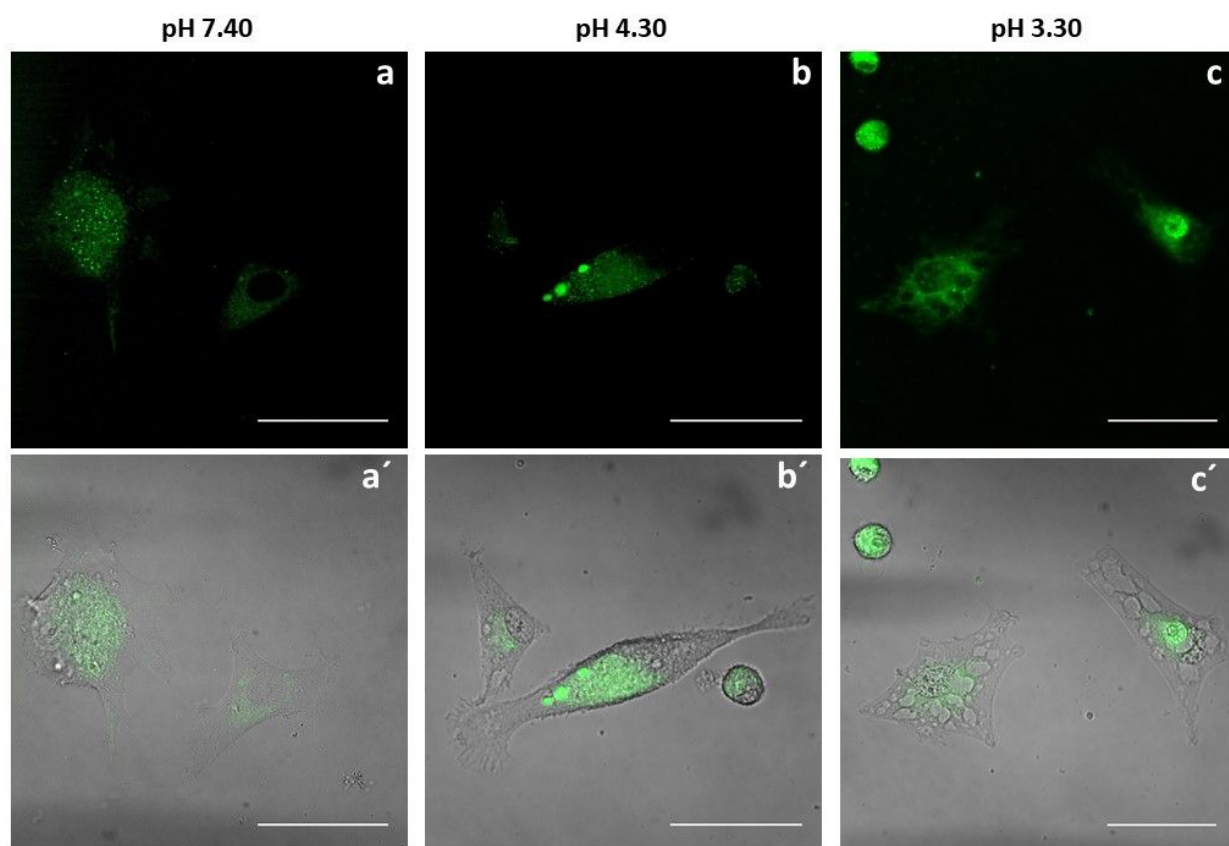


Figure S11. (a-c) Fluorescence images of probe **4b** (10⁻⁵ M, TP excitation: $\lambda_{\text{exc}} = 800$ nm, $\lambda_{\text{em}} = 500$ -550 nm) and (a'-c') merged with the brightfield in MEF cells at different pH values (7.40, 4.30 and 3.30). Scale bar: 50 μm .

11. Co-localisation Experiments.

Co-localisation experiments were performed by adding LysoTracker Deep Red (ThermoFisher Scientific Cat. No. L12492; 50 nM final concentration) to the cell culture media approximately 30 minutes prior to visualisation by microscopy. LysoTracker was visualised using single photon excitation (633 nm excitation/709-791 nm detection). Compound **4b** or **4c** were detected sequentially using the two-photon configuration described in the Experimental Section. As lysosomes are extremely mobile in MEF cells, images were captured at high speed to minimise the time delay between confocal and two-photon acquisitions (<1 s). Identical laser power and gain settings were used for all samples within each experiment.

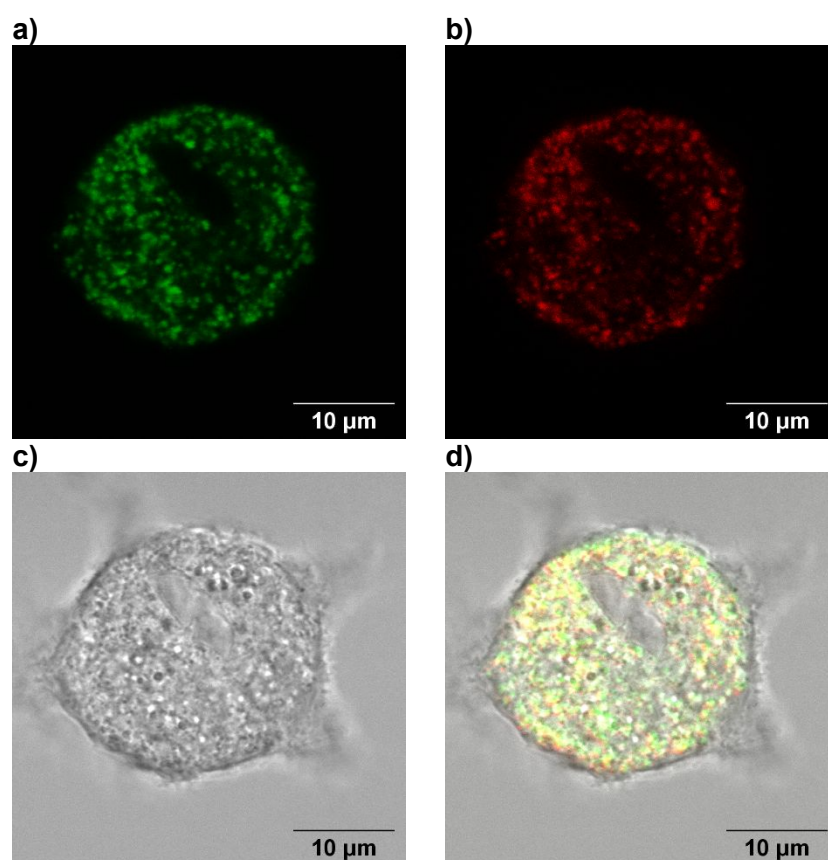


Figure S12: MEF cells incubated (a) with **4c** (10 μM) (b) LysoTracker Deep Red (50 nM). (c) Bright field. (d) Merge images.

12. NMR spectra.

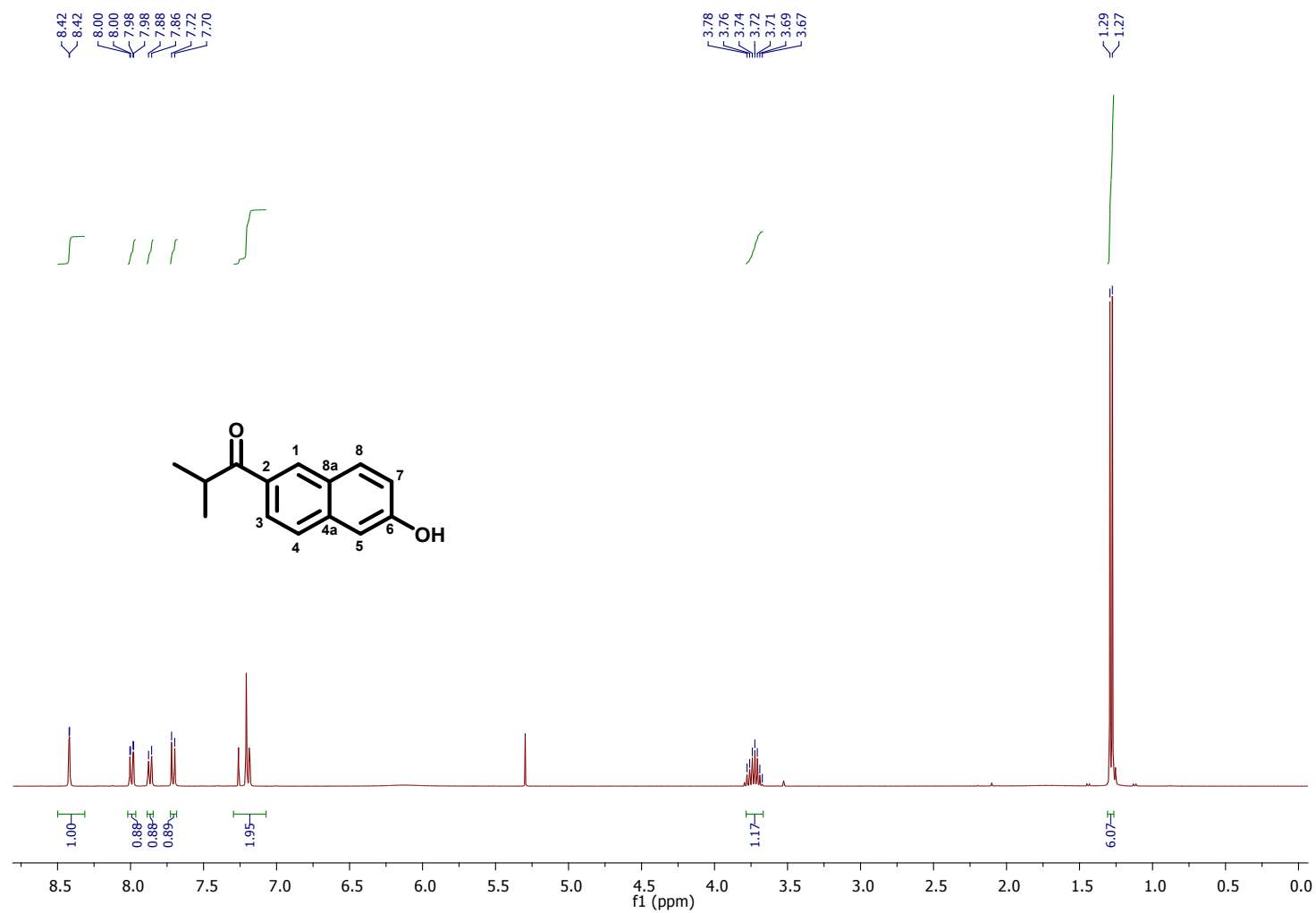


Figure S13: ^1H -NMR spectrum of compound **2** in CDCl_3

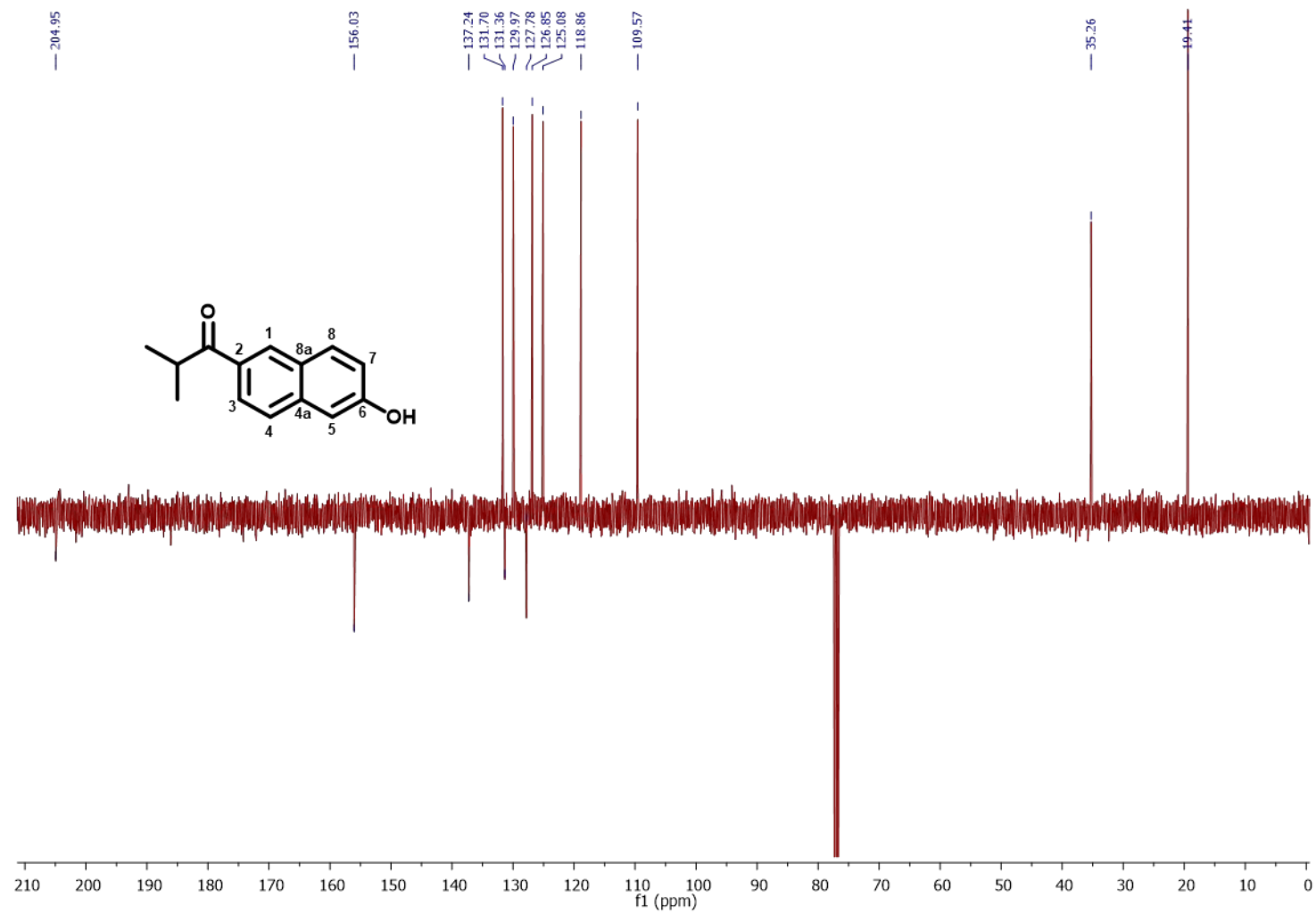


Figure S14: ¹³C-NMR spectrum of compound **2** in CDCl₃

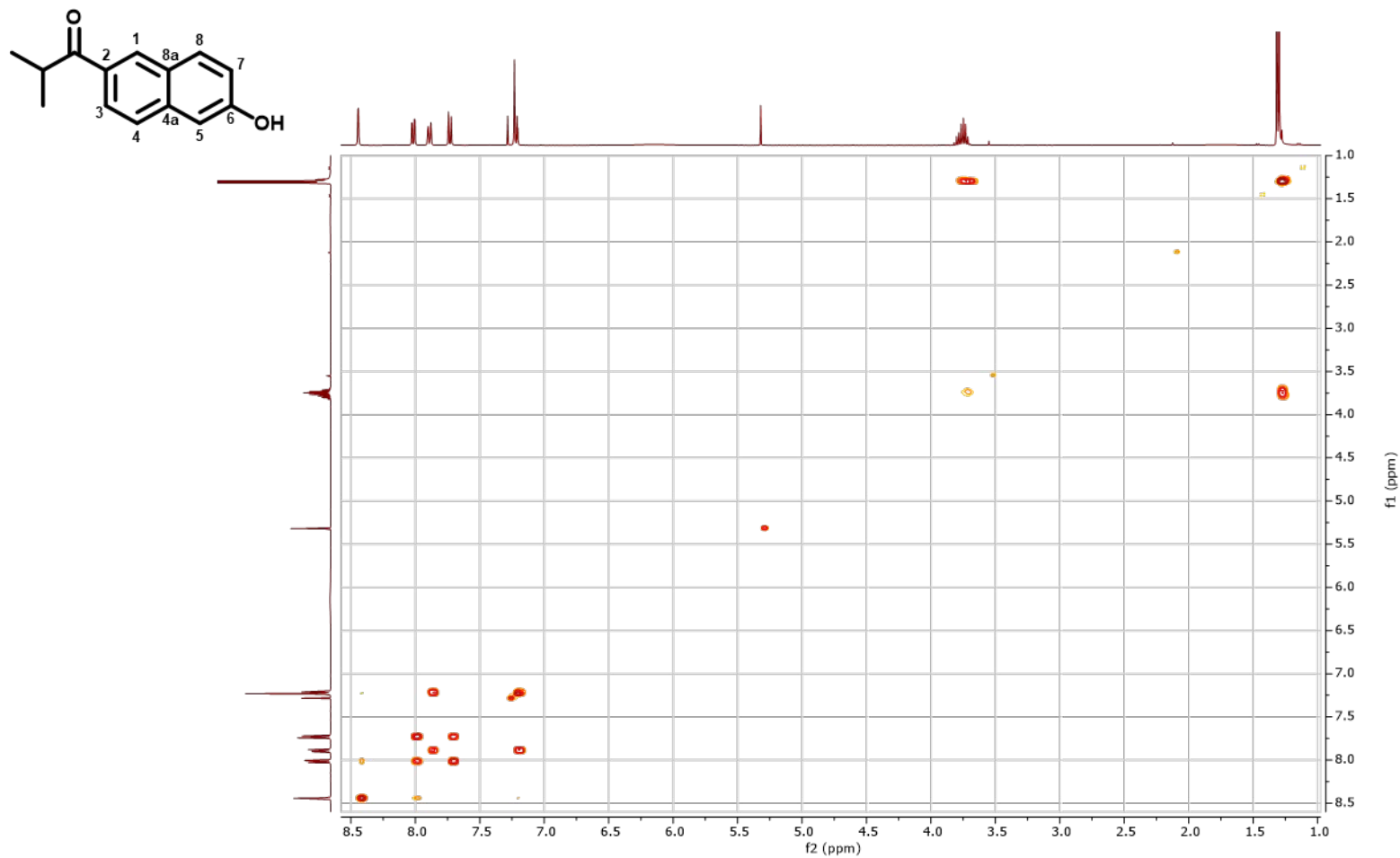


Figure S15: ^1H - ^1H -COSY spectrum of compound **2** in CDCl_3

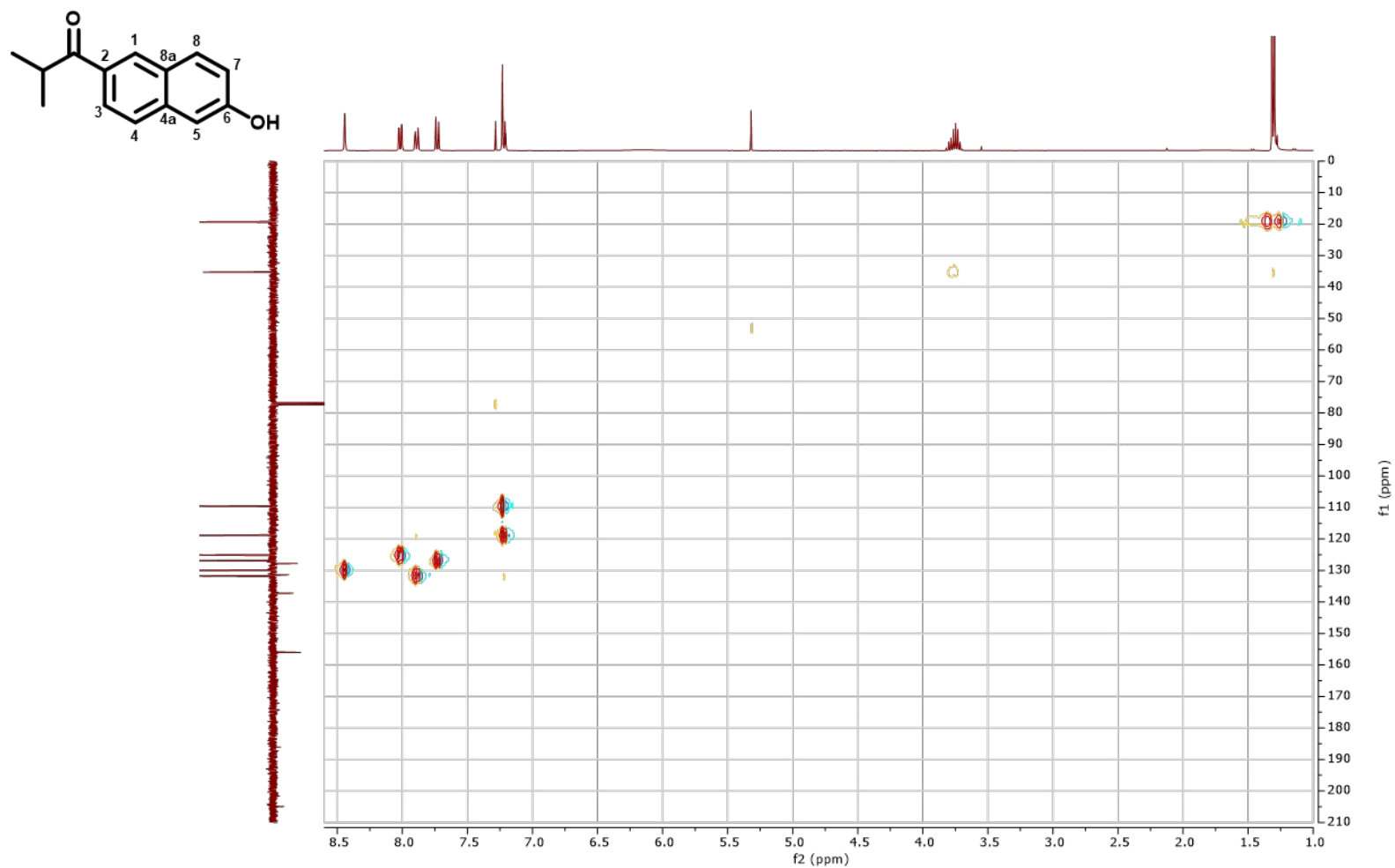


Figure S16: ^1H - ^{13}C -HSQC spectrum of compound **2** in CDCl_3

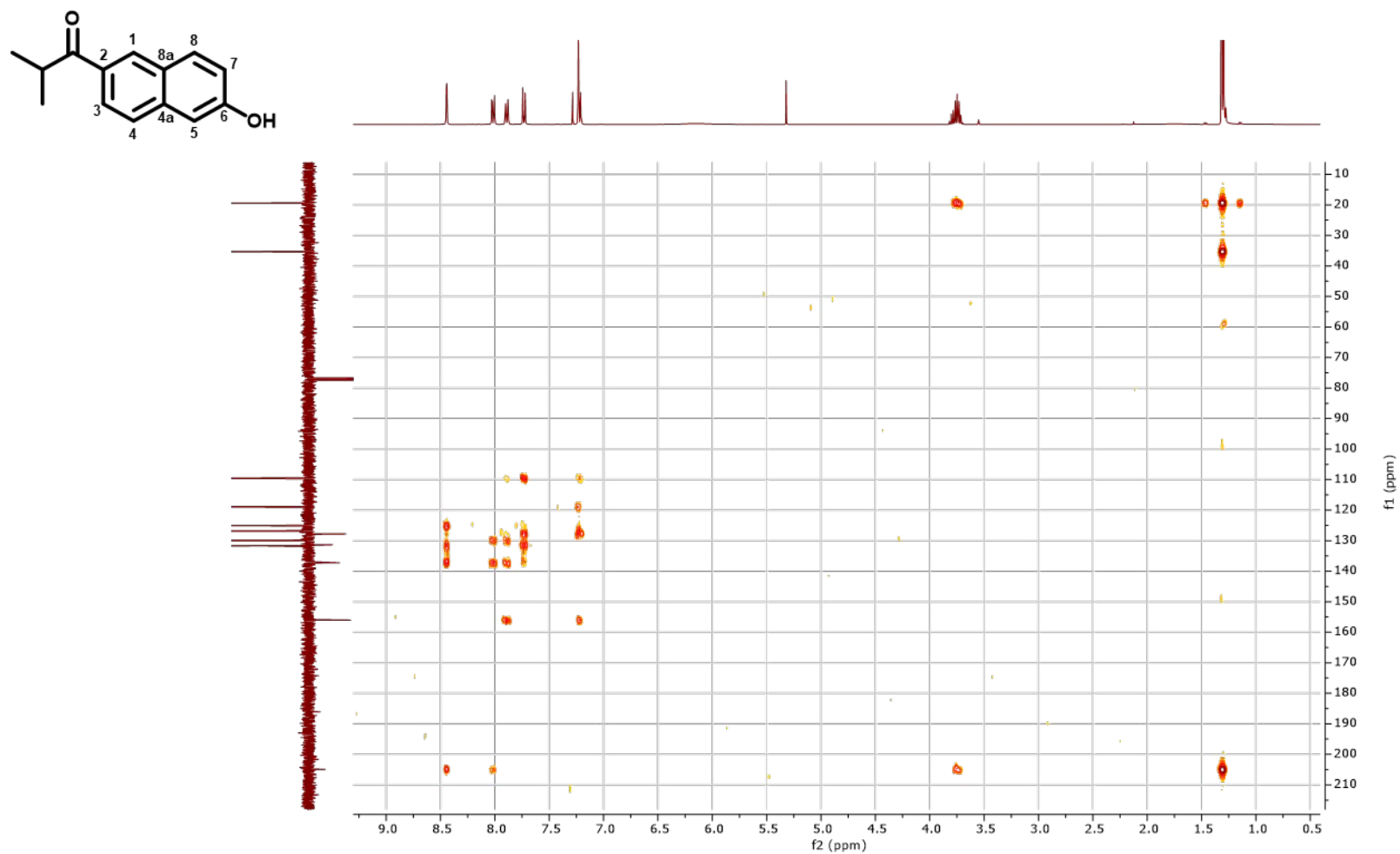


Figure S17: ^1H - ^{13}C -HMBC spectrum of compound **2** in CDCl_3

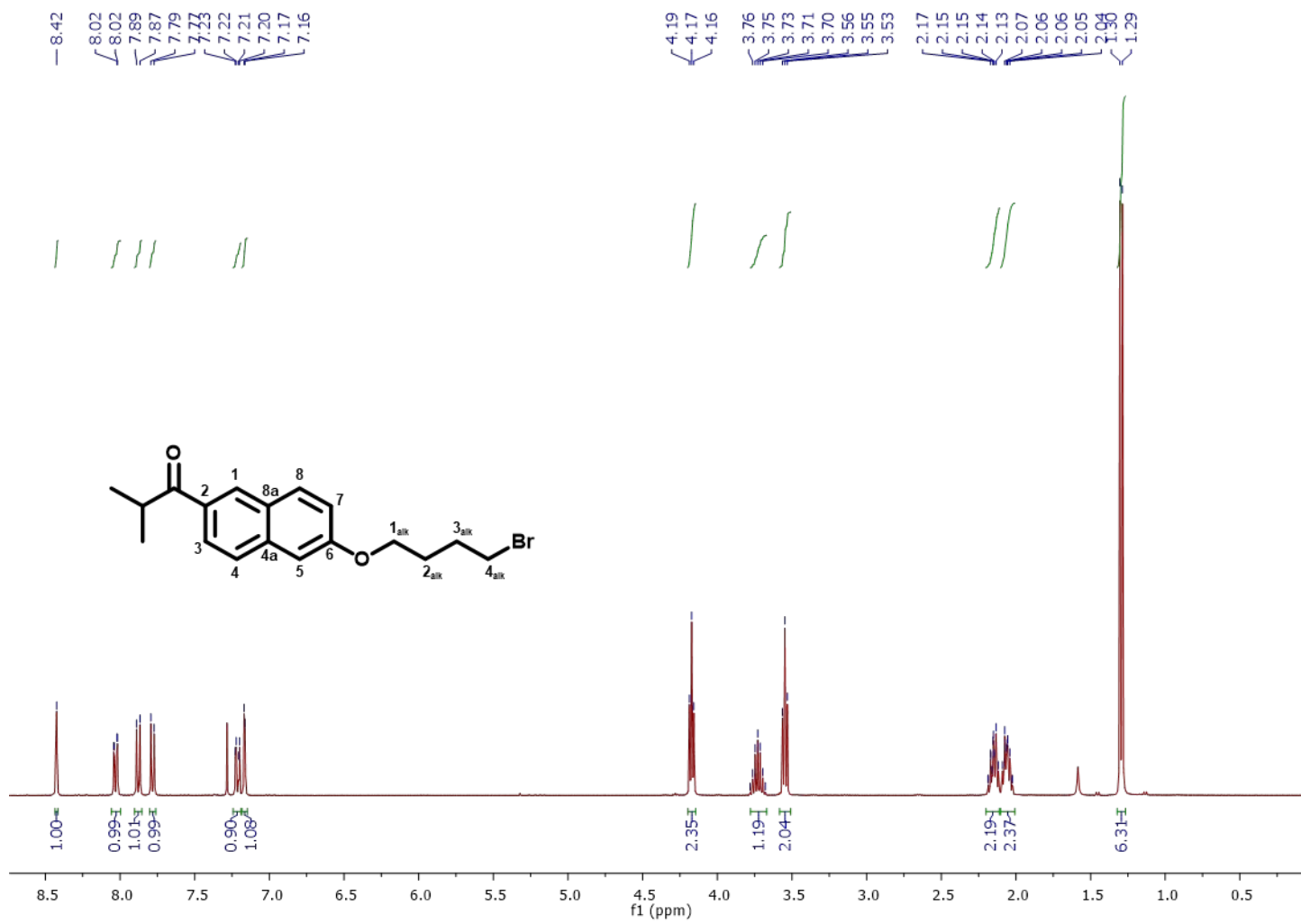


Figure S18: ¹H-NMR spectrum of compound **3a** in CDCl₃

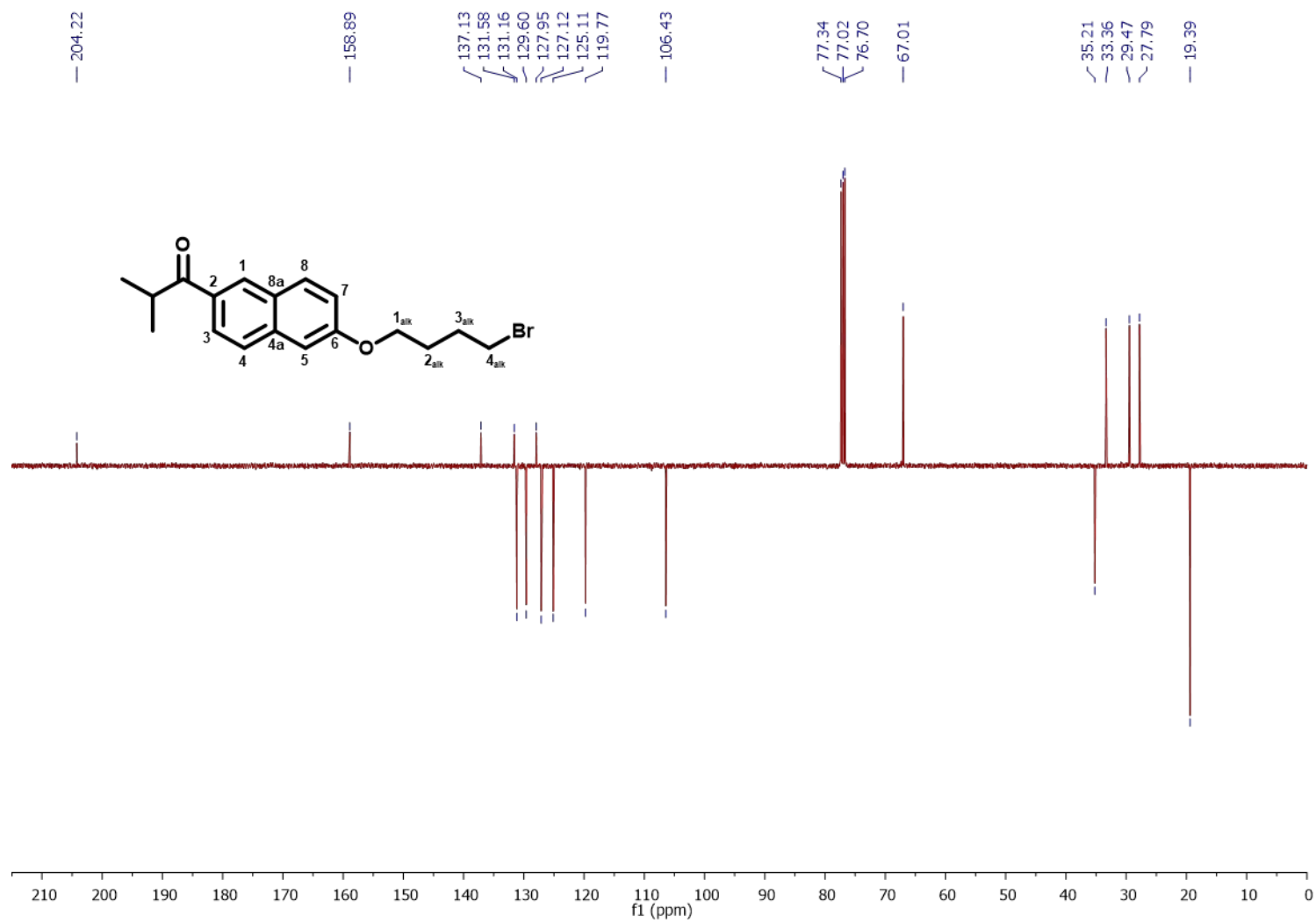


Figure S19: ¹³C-NMR spectrum of compound **3a** in CDCl₃

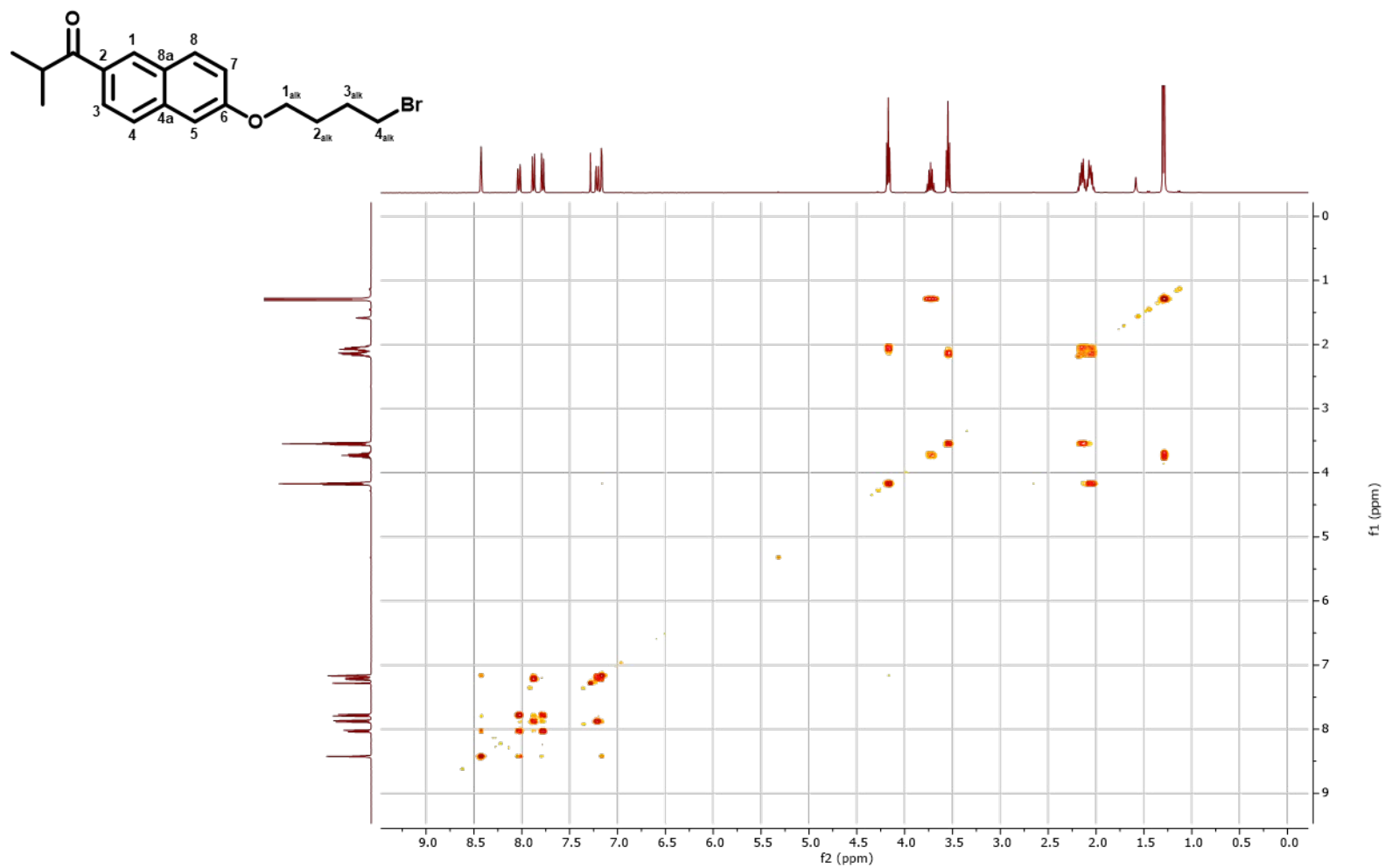


Figure S20: ^1H - ^1H -COSY spectrum of compound **3a** in CDCl_3

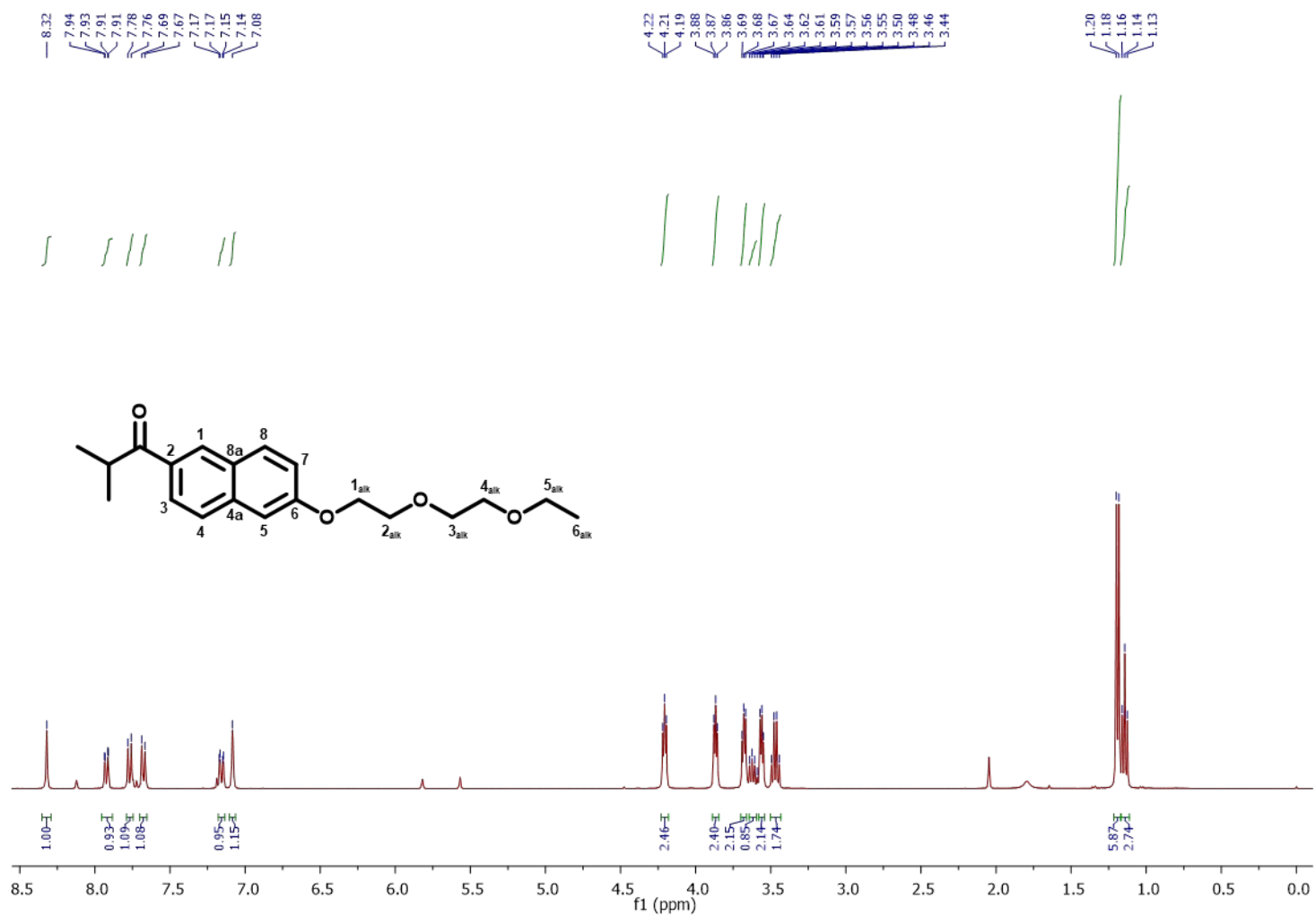


Figure S21: ^1H -NMR spectrum of compound **3b** in CDCl_3

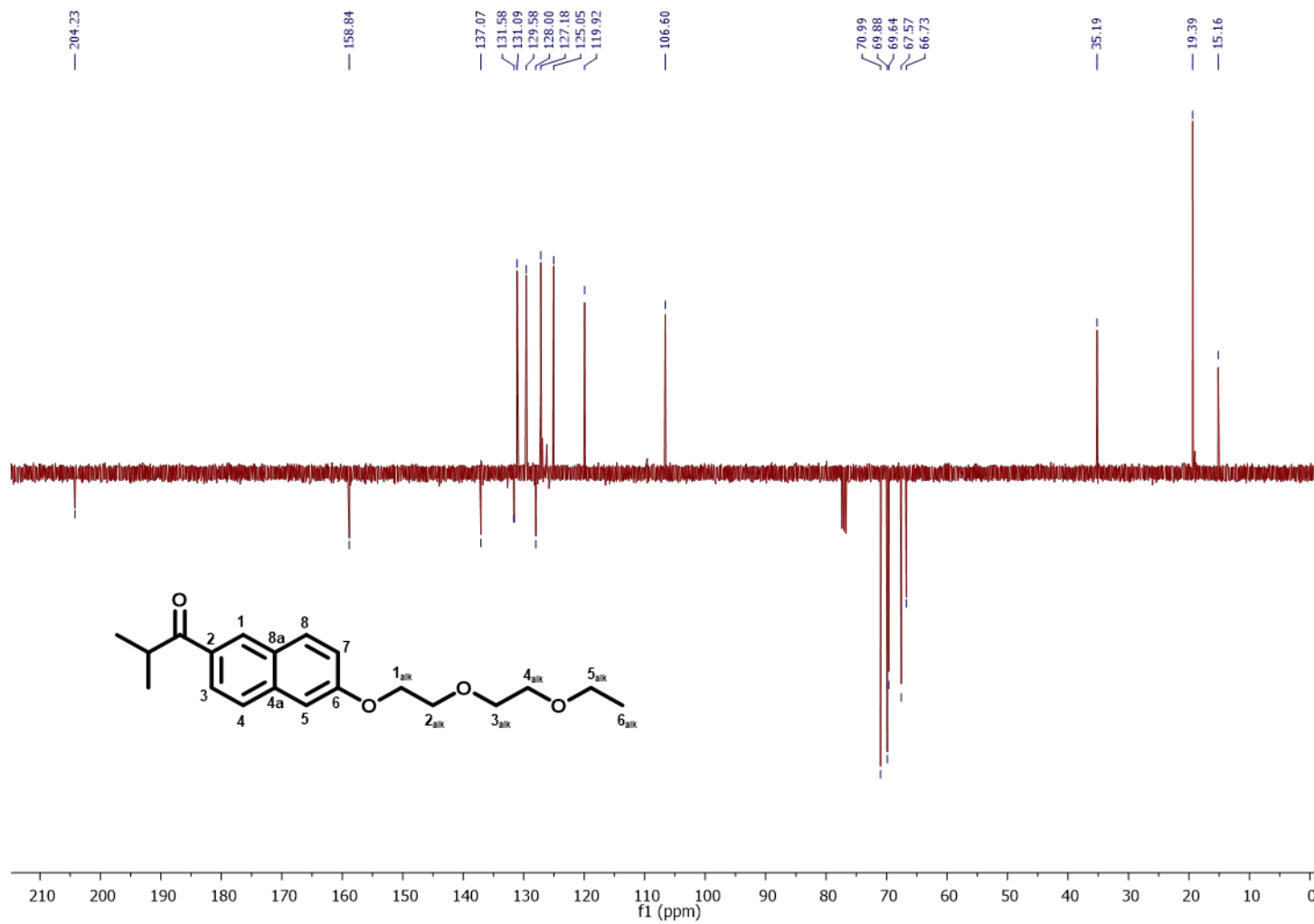


Figure S22: ¹³C-NMR spectrum of compound **3b** in CDCl₃

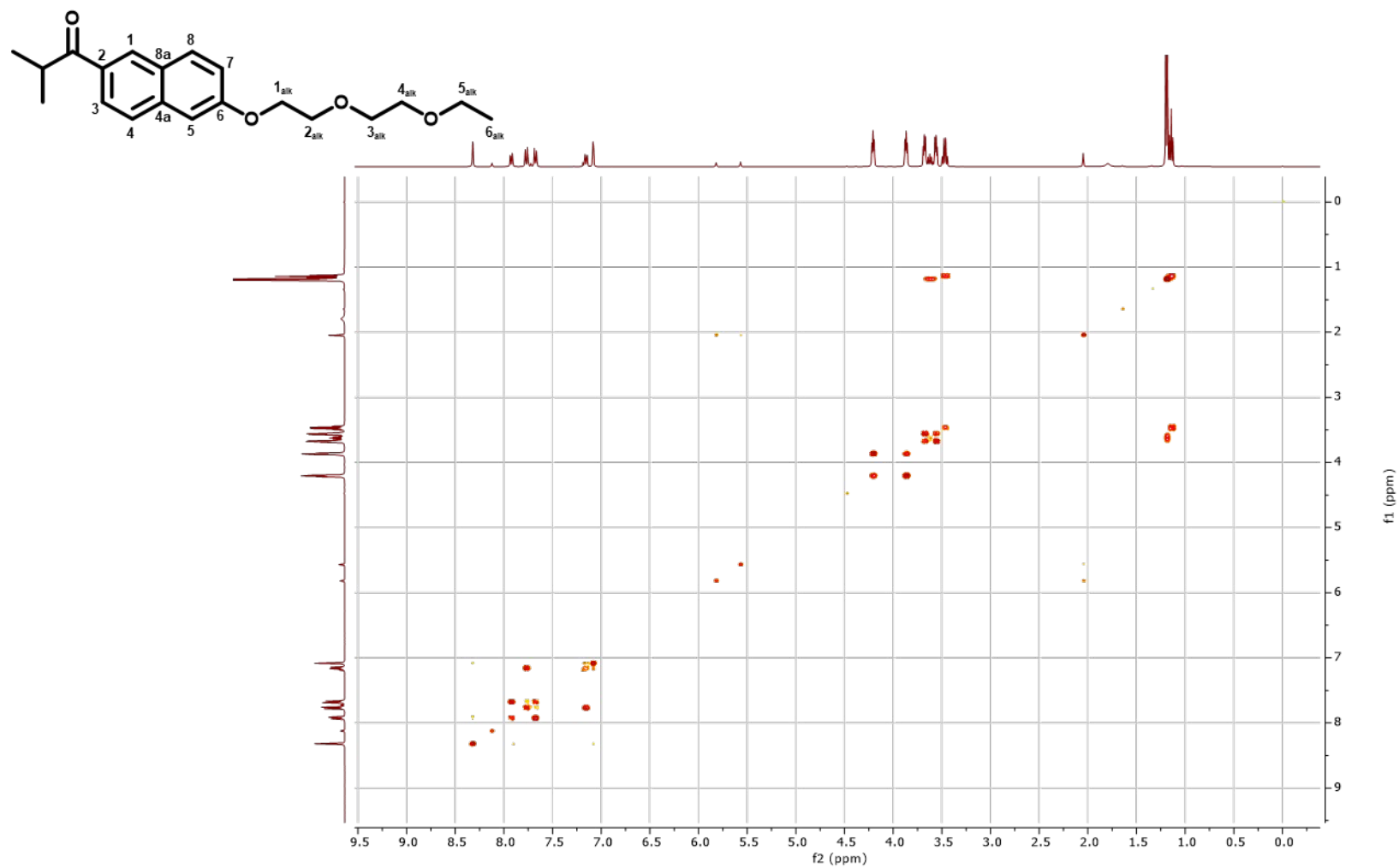


Figure S23: ¹H-¹H-COSY spectrum of compound **3b** in CDCl₃

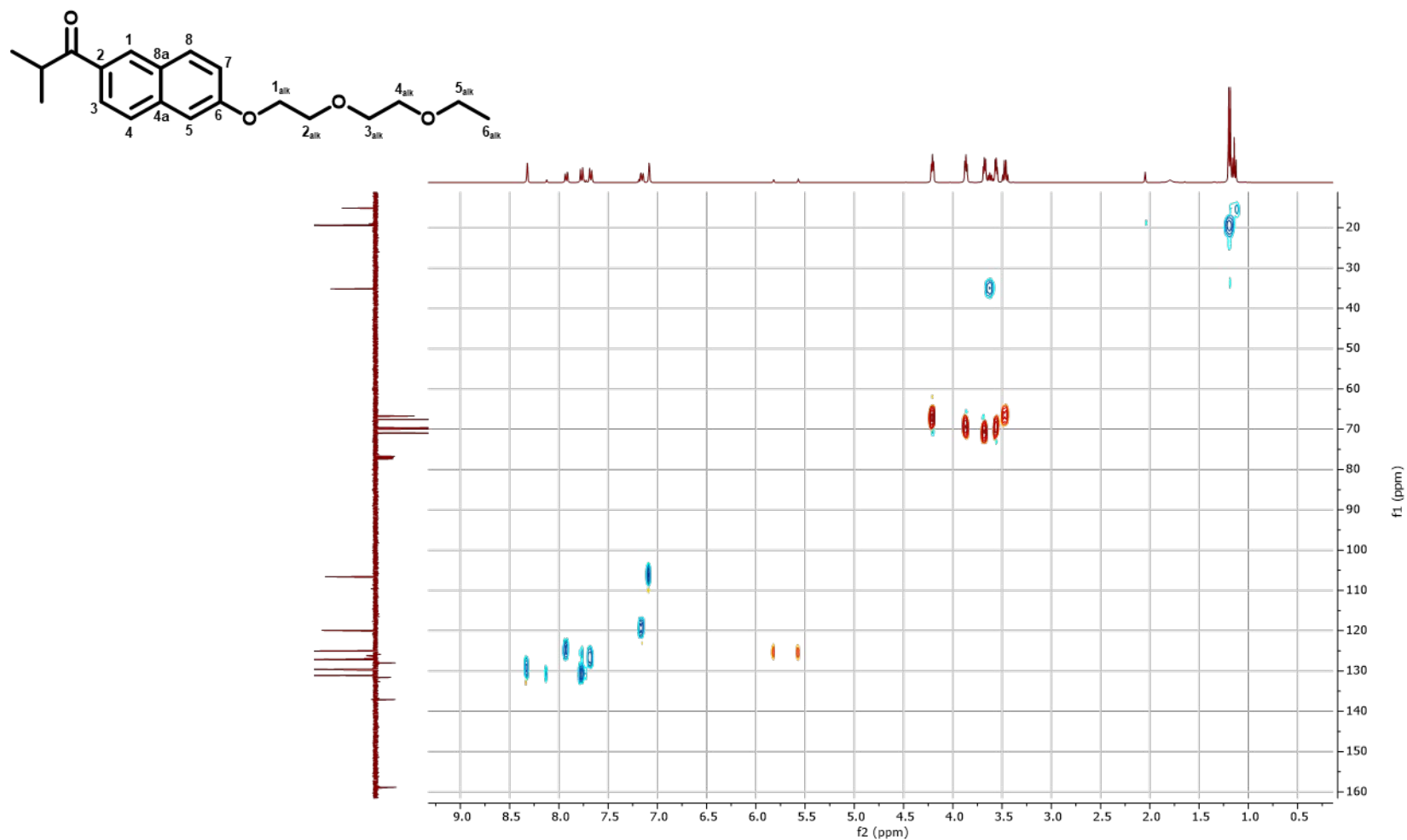


Figure S24: ^1H - ^{13}C -HSQC spectrum of compound **3b** in CDCl_3

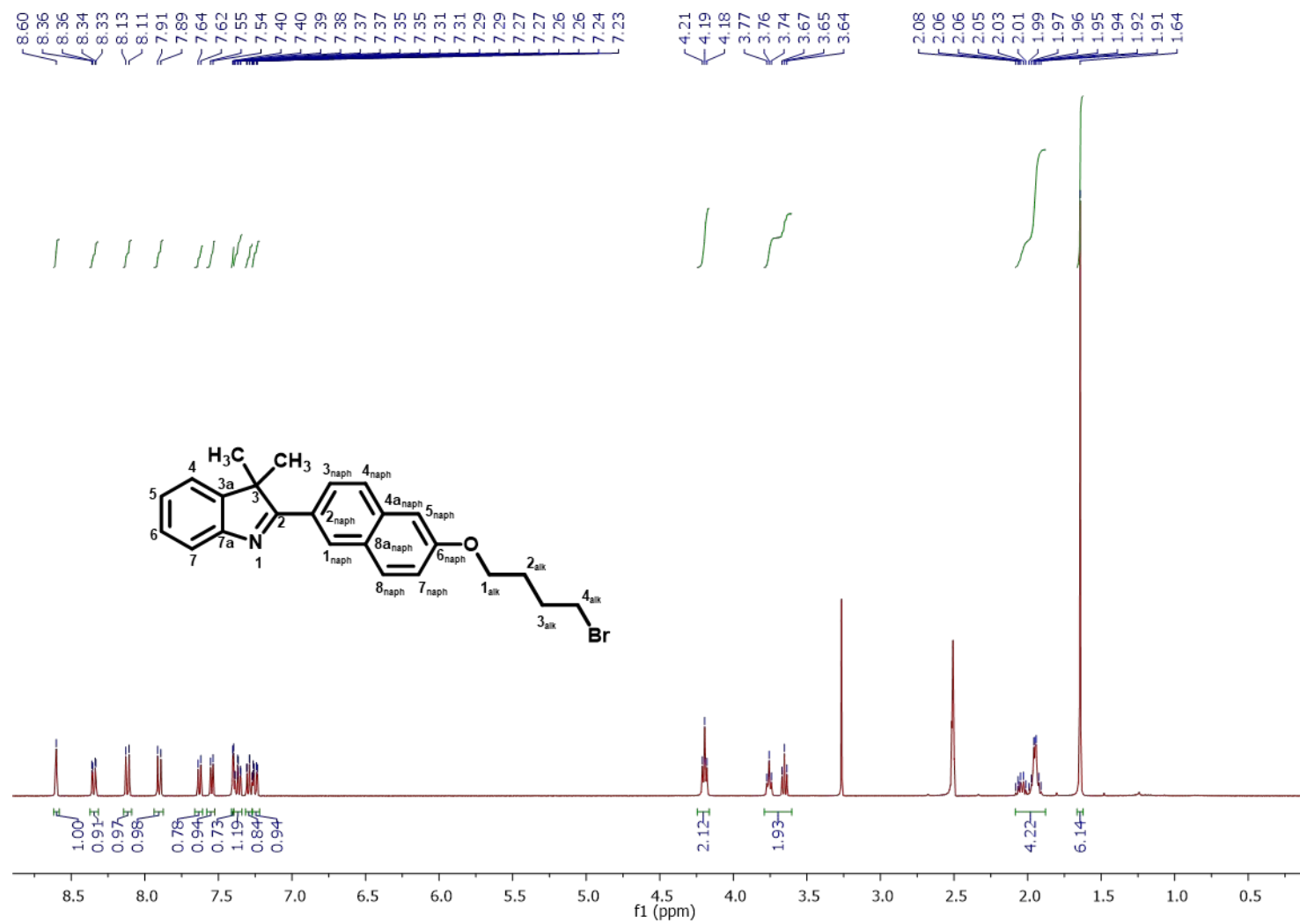


Figure S25: ¹H-NMR spectrum of compound **4a** in DMSO-*d*₆

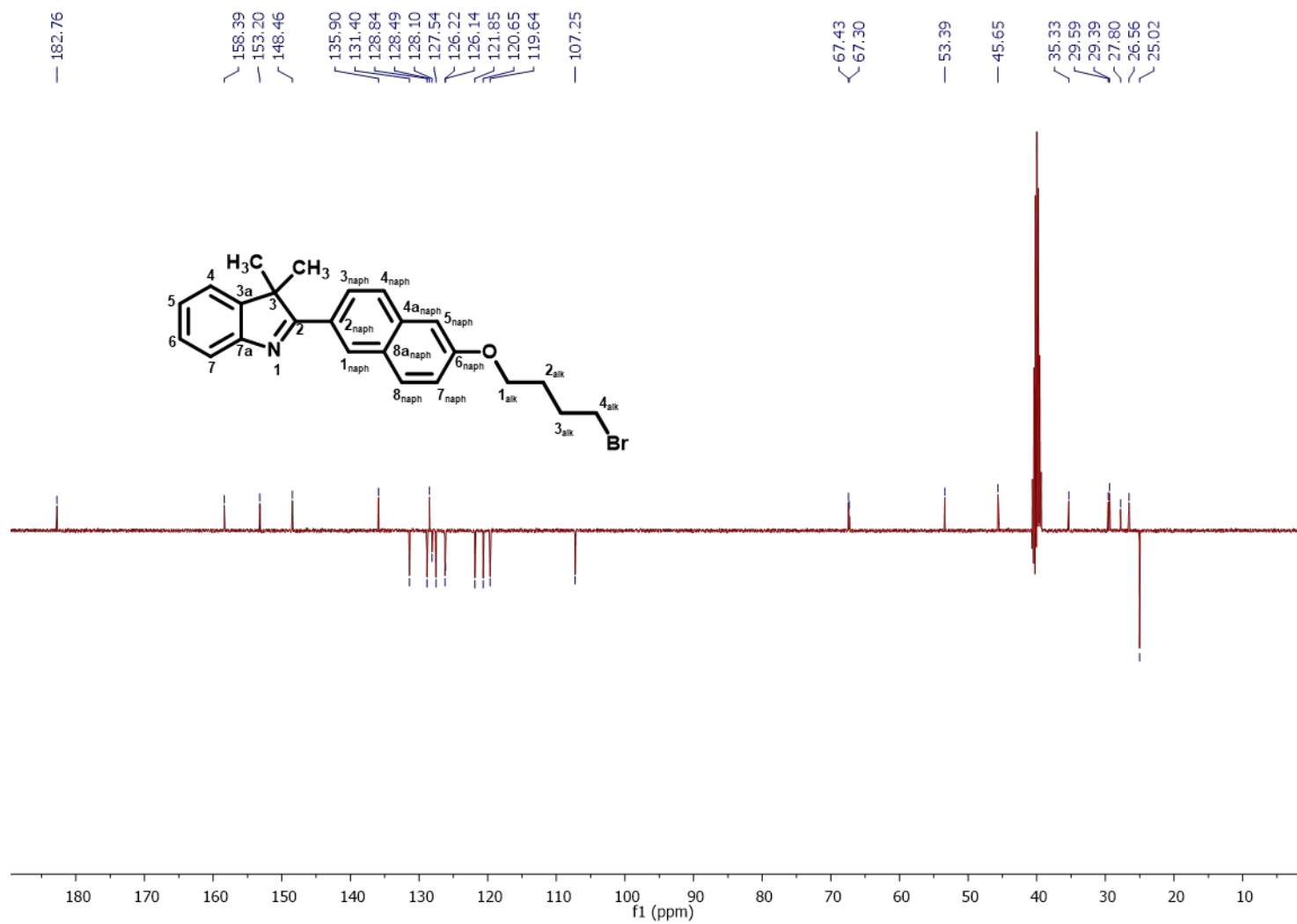


Figure S26: ¹³C-NMR spectrum of compound **4a** in DMSO-*d*₆

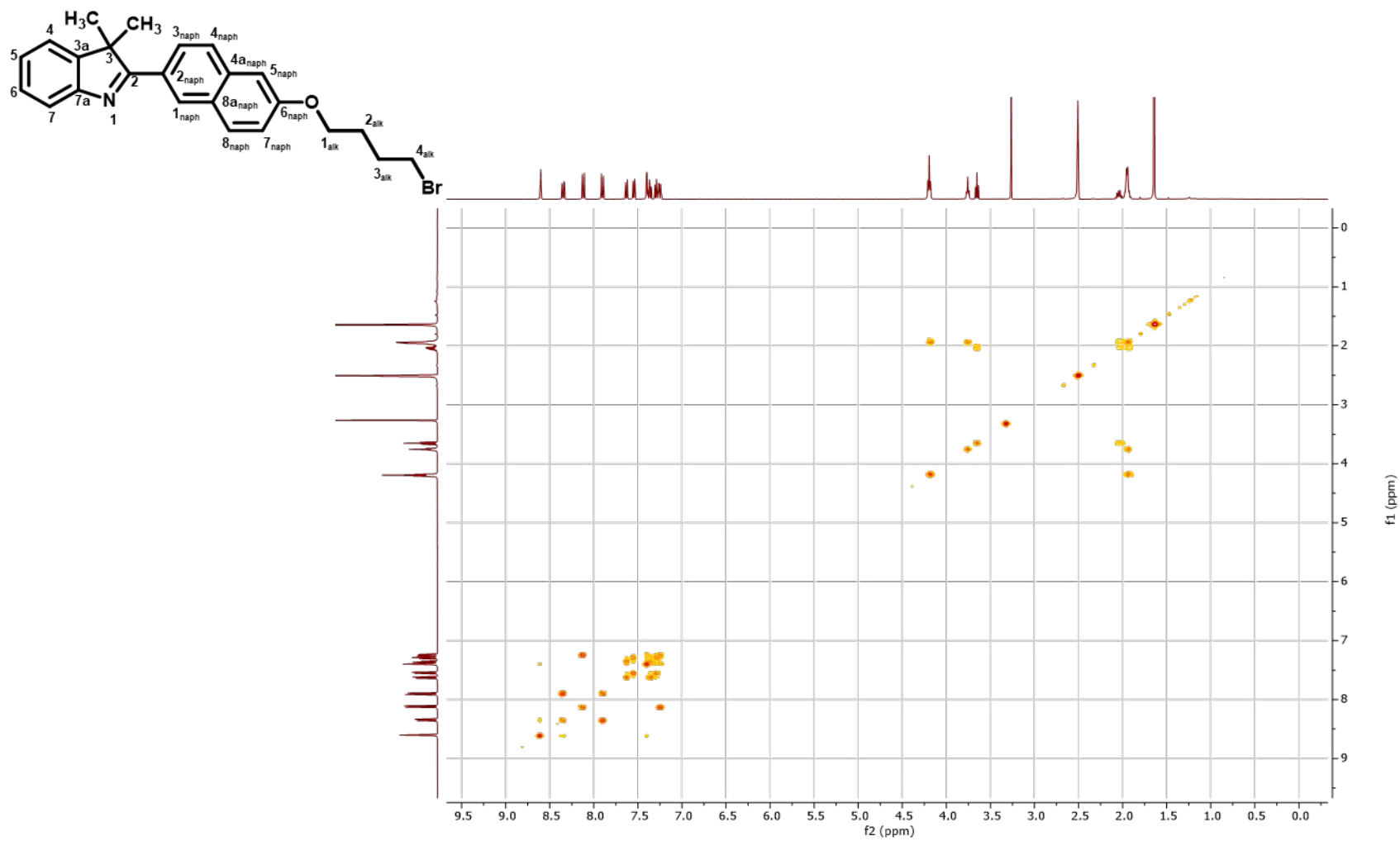


Figure S27: ¹H-¹H-COSY spectrum of compound **4a** in DMSO-*d*₆

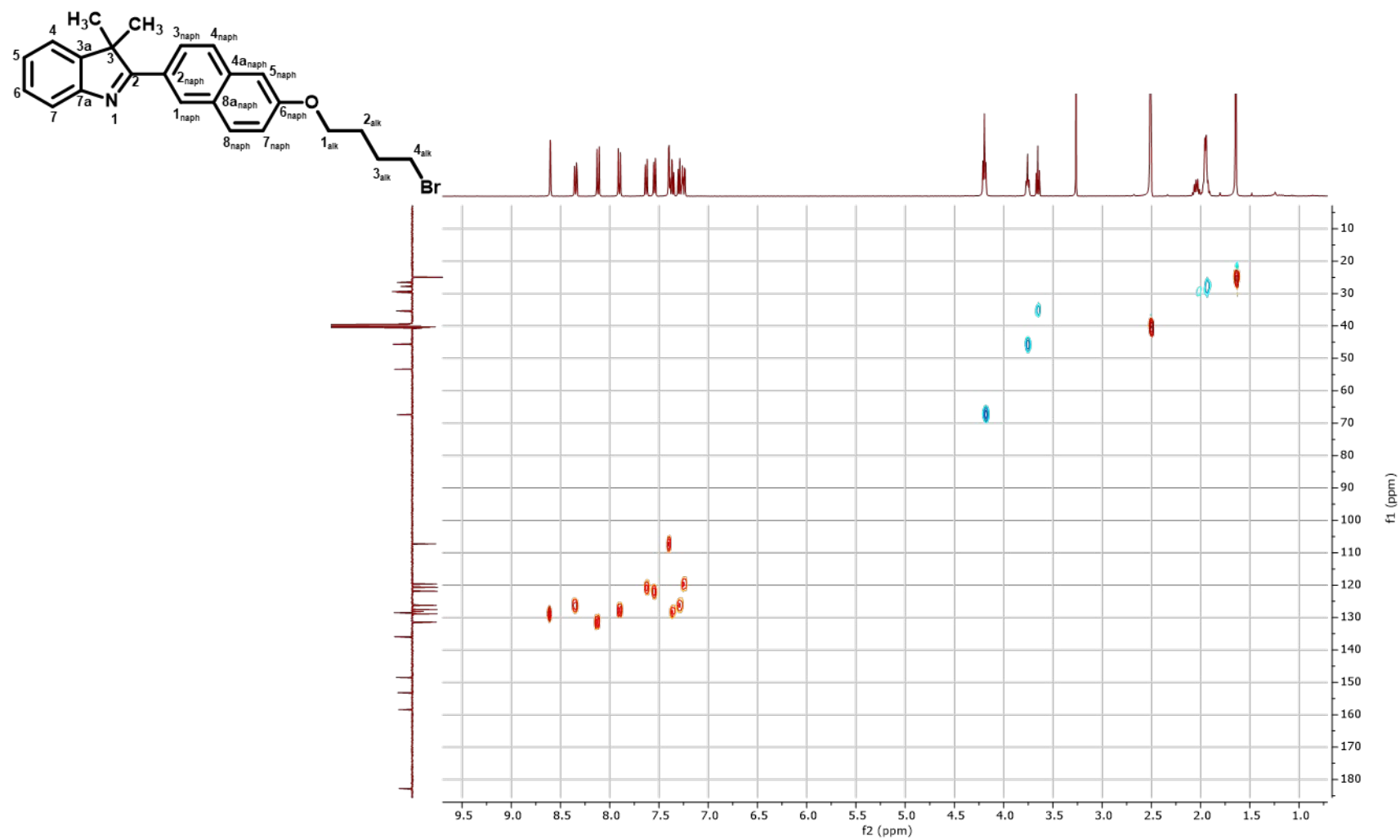


Figure S28: ^1H - ^{13}C -HSQC spectrum of compound **4a** in $\text{DMSO}-d_6$

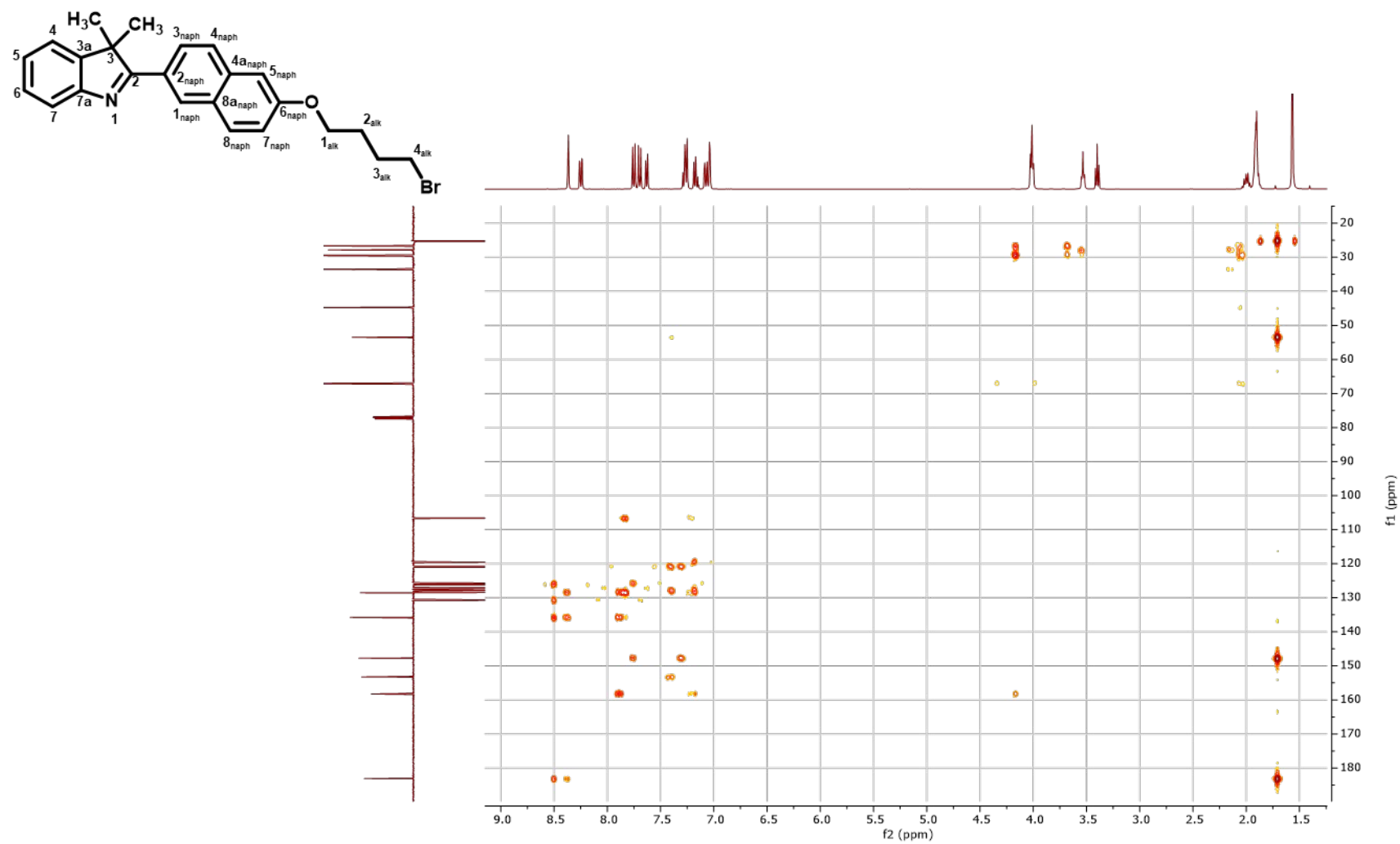


Figure S29: ^1H - ^{13}C -HMBC spectrum of compound **4a** in $\text{DMSO}-d_6$

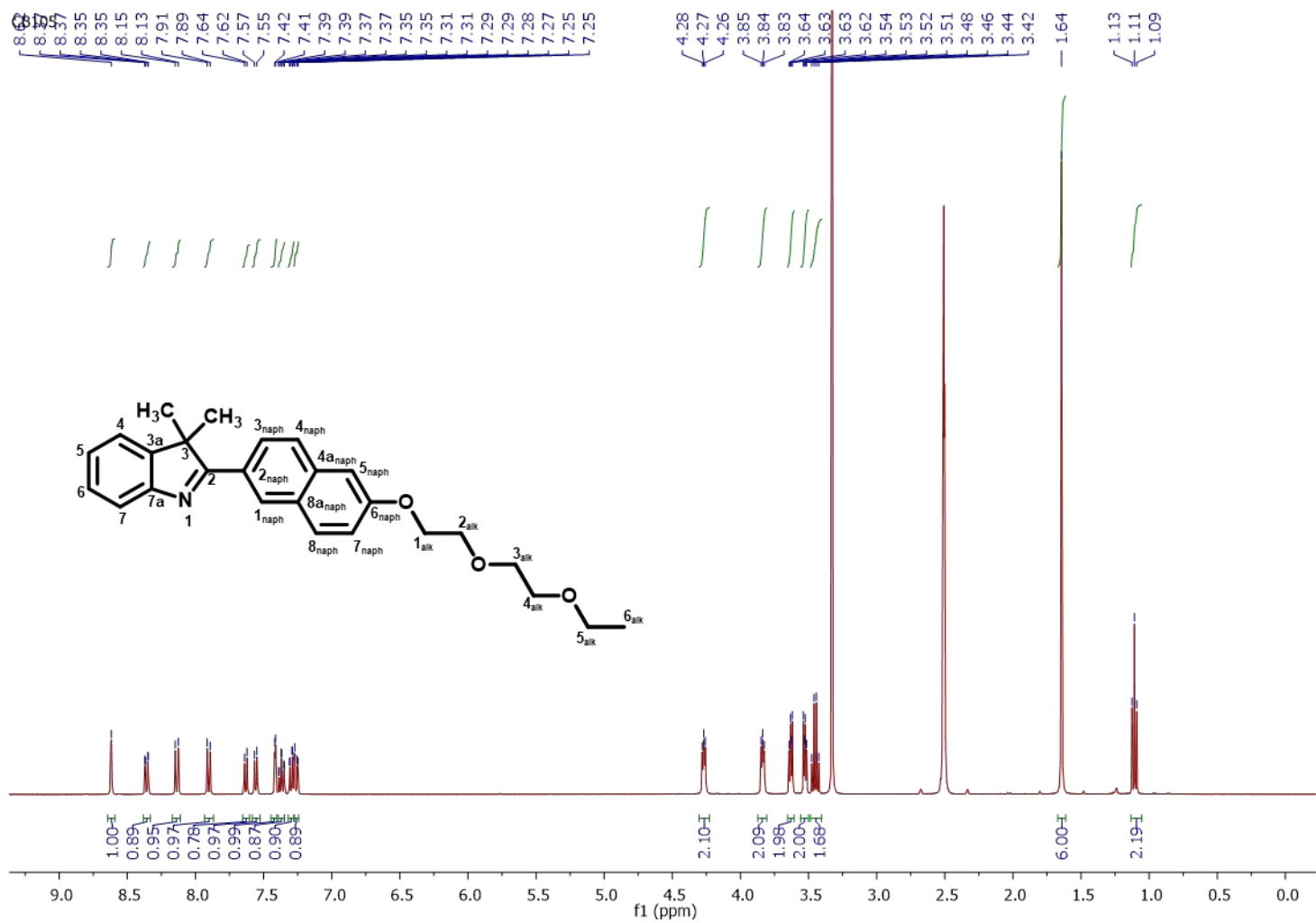


Figure S30: ¹H-NMR spectrum of compound **4b** in DMSO-*d*₆

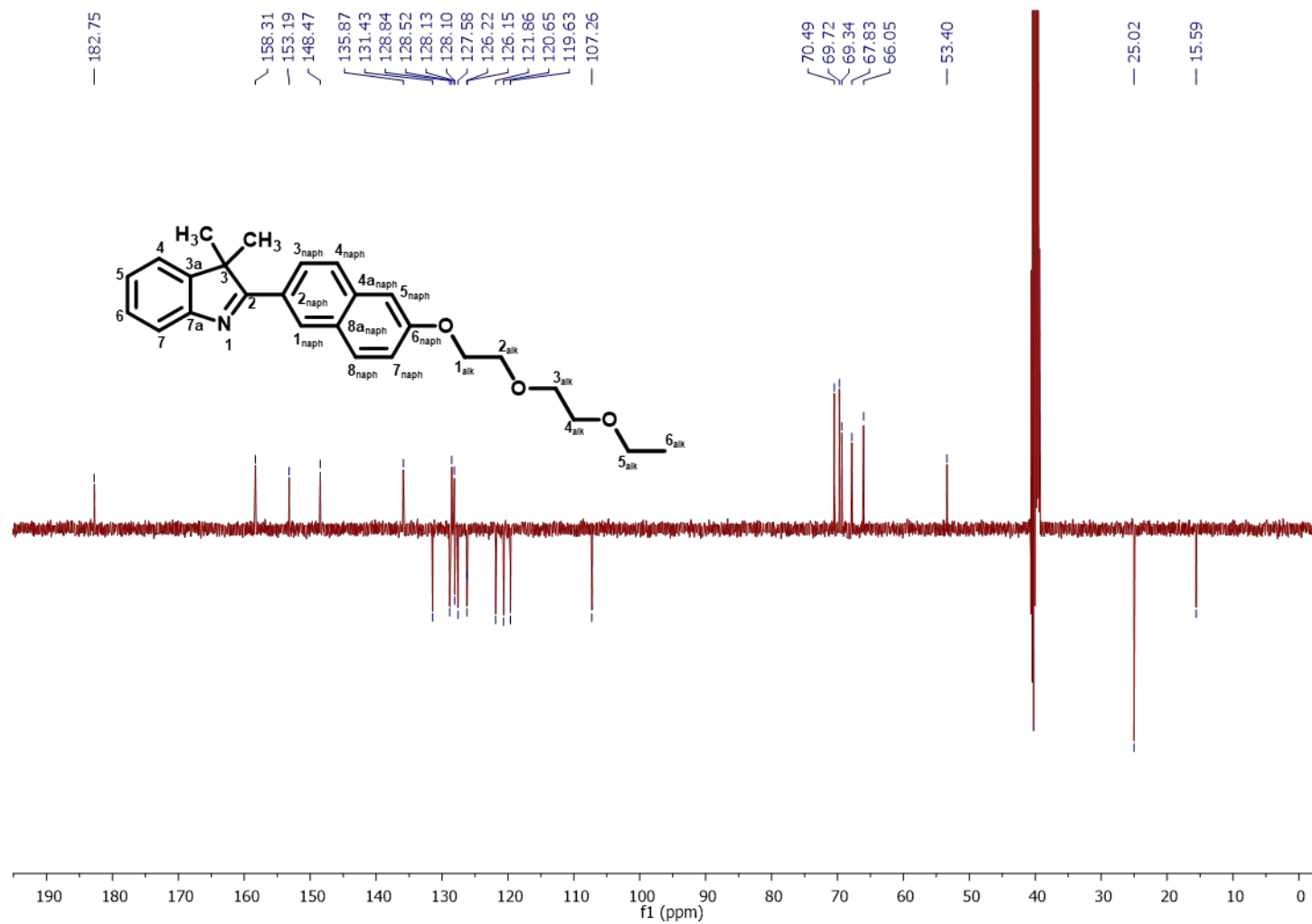


Figure S31: ^{13}C -NMR spectrum of compound **4b** in $\text{DMSO}-d_6$

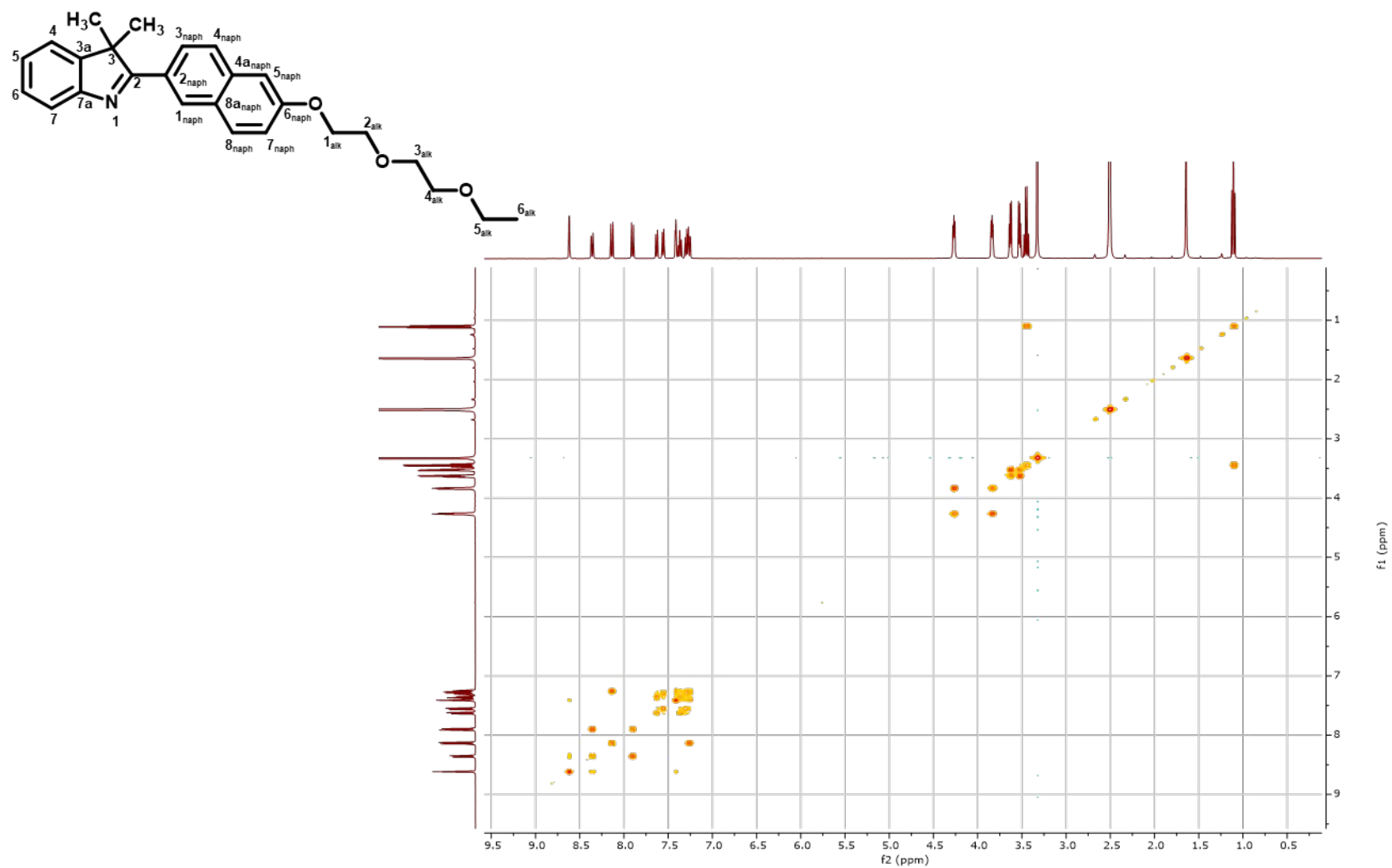


Figure S32: ¹H-¹H-COSY spectrum of compound **4b** in DMSO-*d*₆

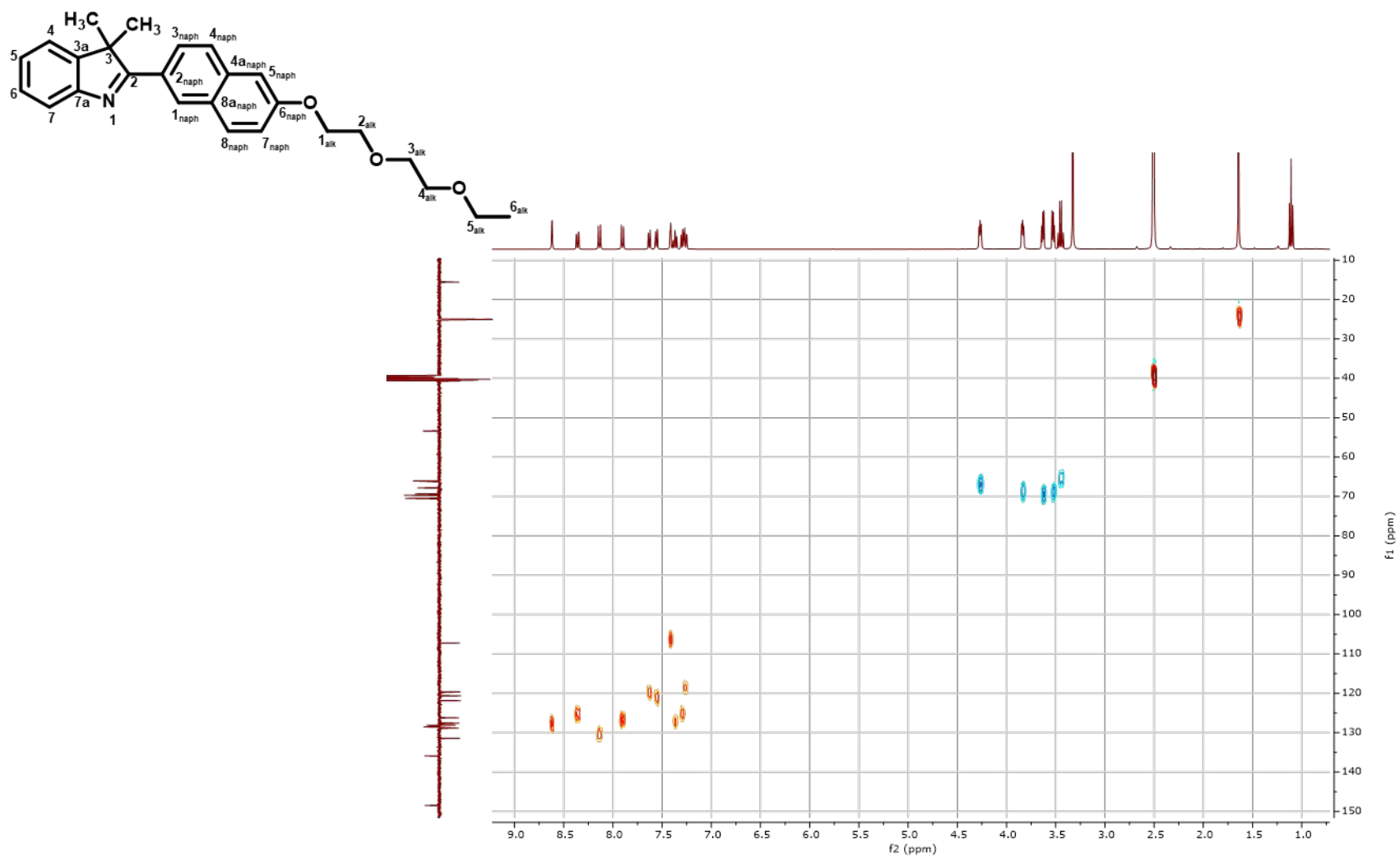


Figure S33: ^1H - ^{13}C -HSQC spectrum of compound **4b** in DMSO- d_6

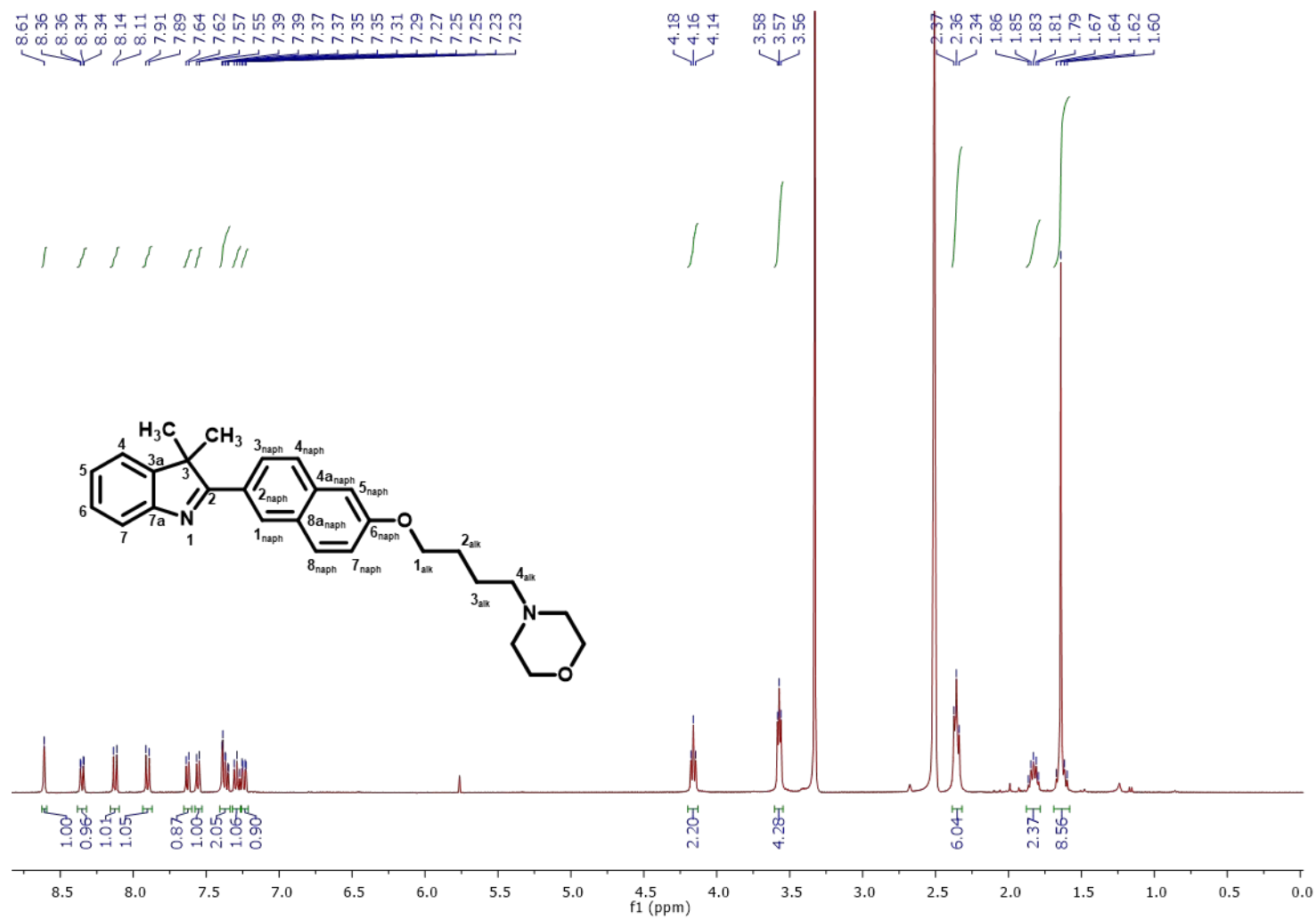


Figure S34: ¹H-NMR spectrum of compound **4c** in DMSO-*d*₆

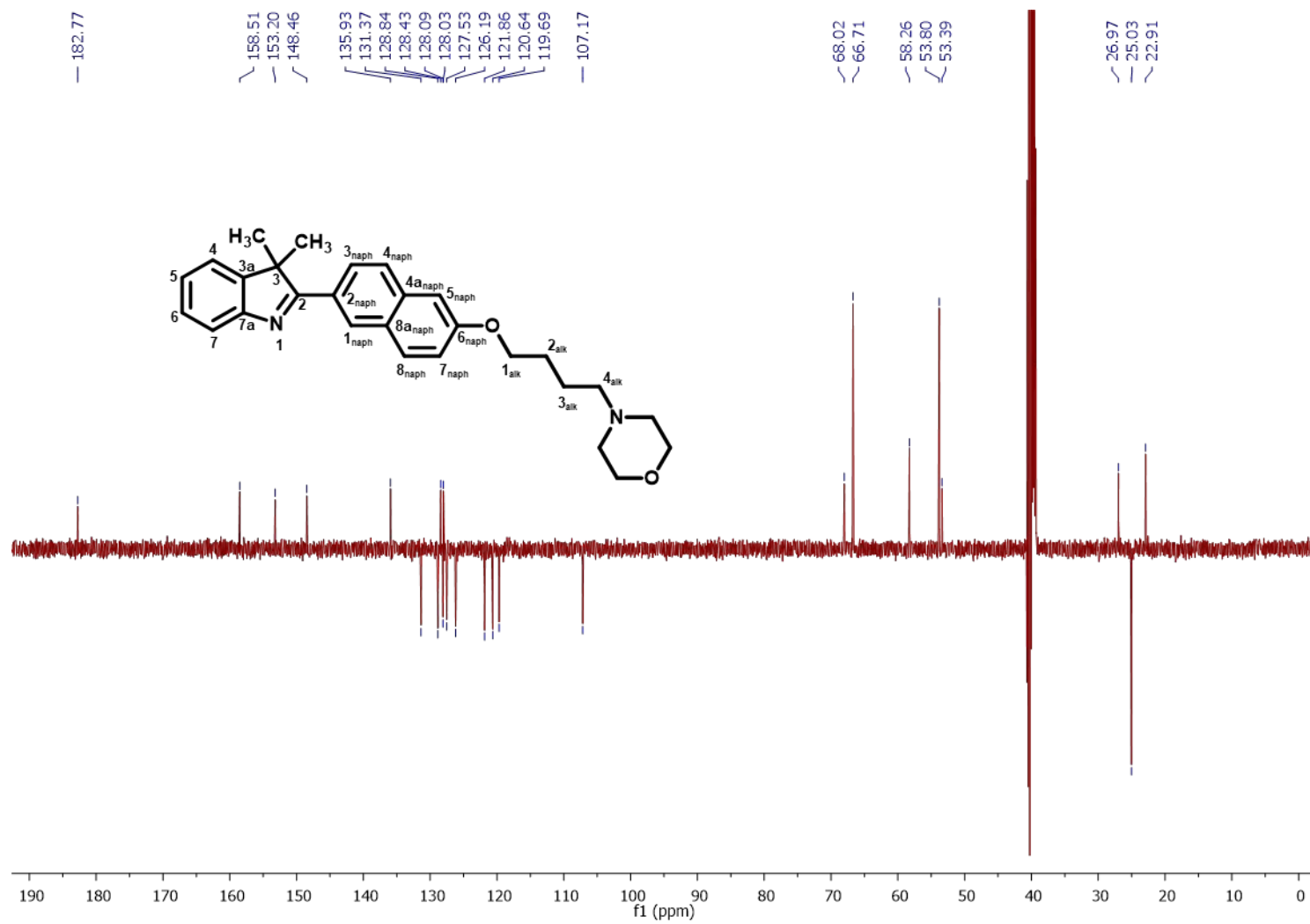


Figure S35: ¹³C-NMR spectrum of compound **4c** in DMSO-*d*₆

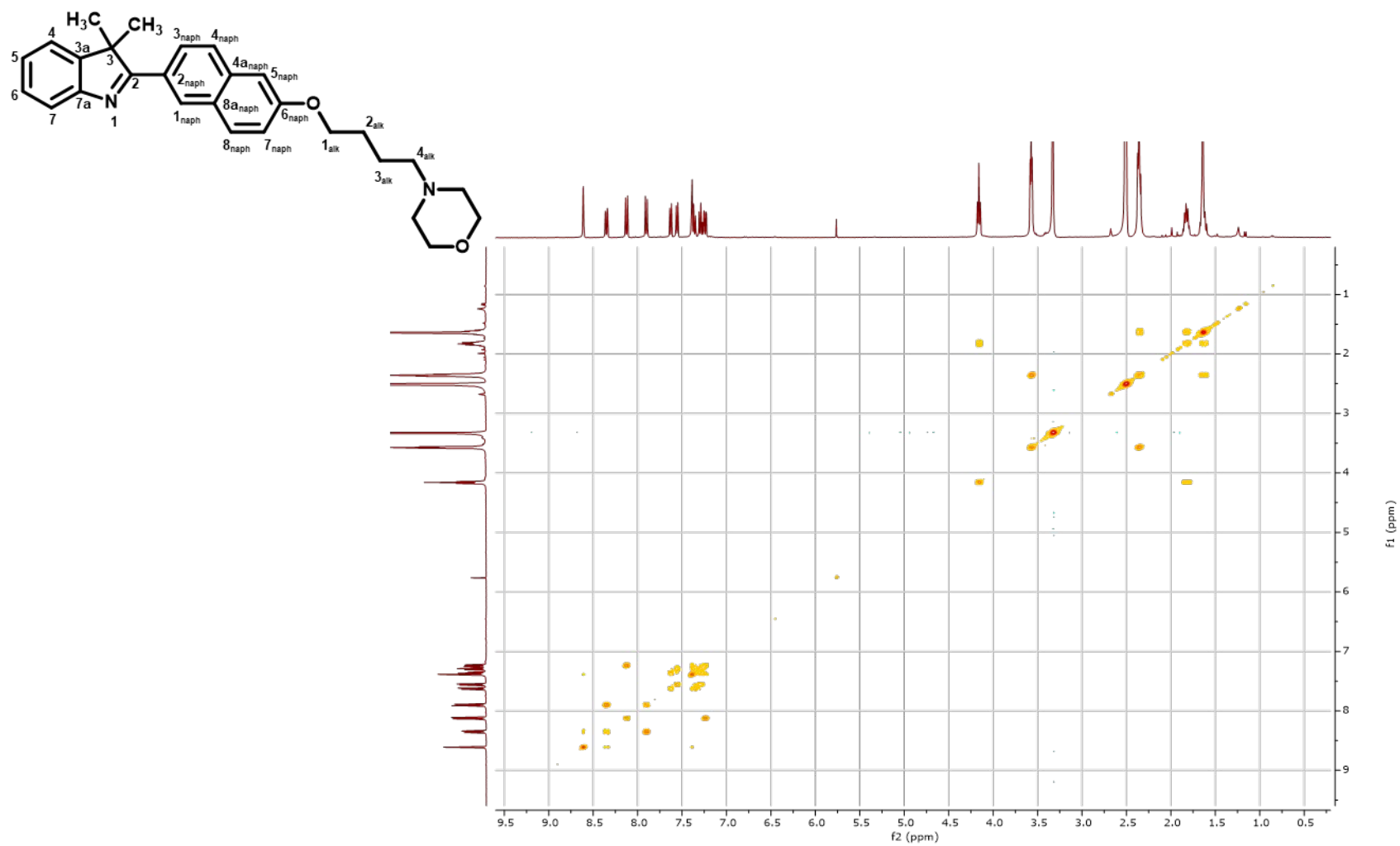


Figure S36: ^1H - ^1H -COSY spectrum of compound **4c** in $\text{DMSO}-d_6$

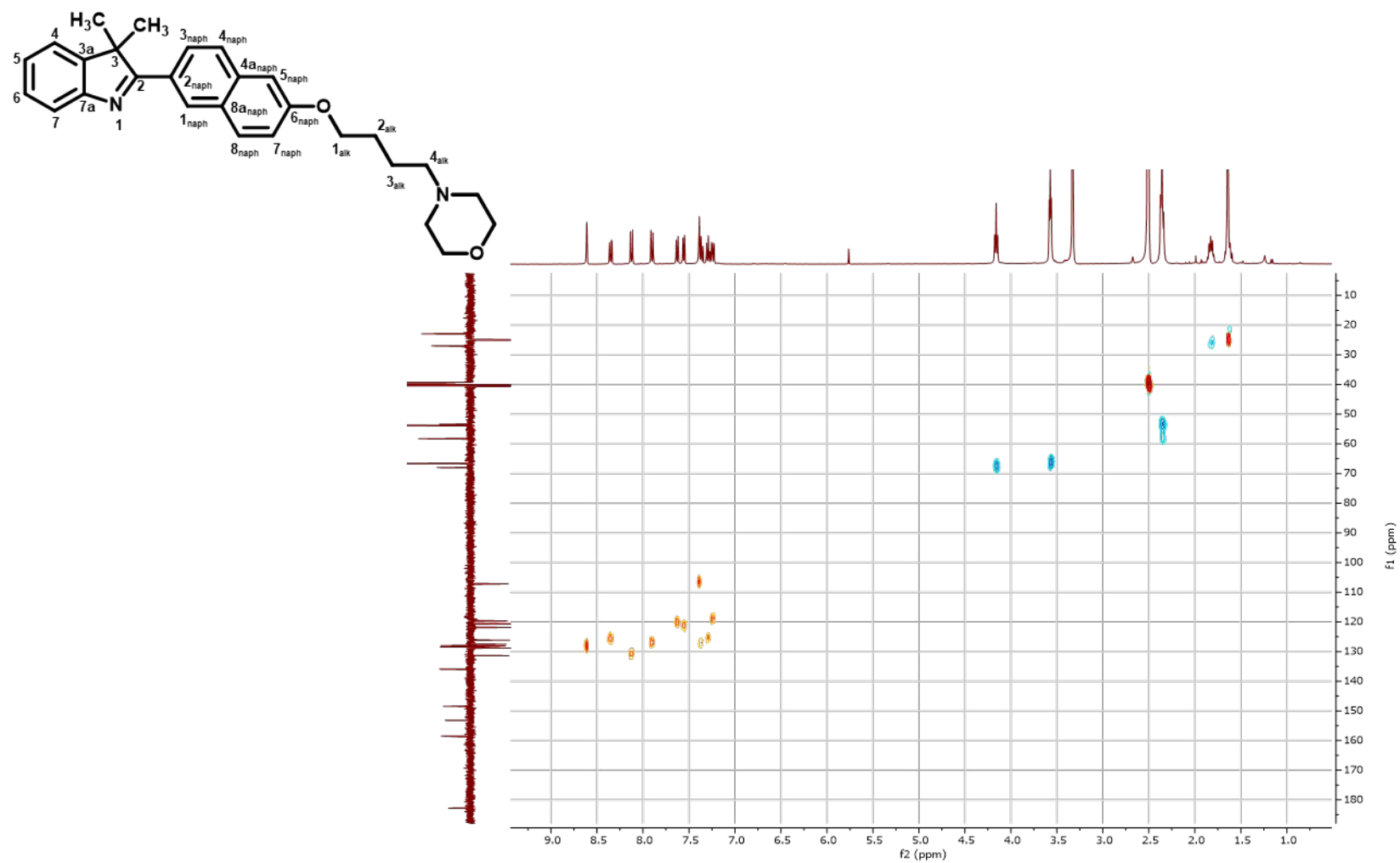
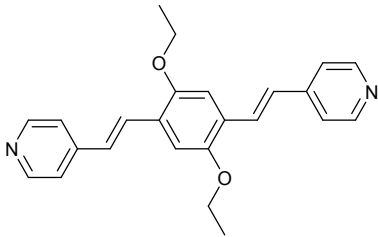
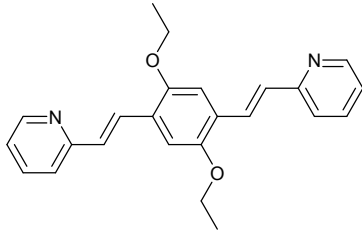
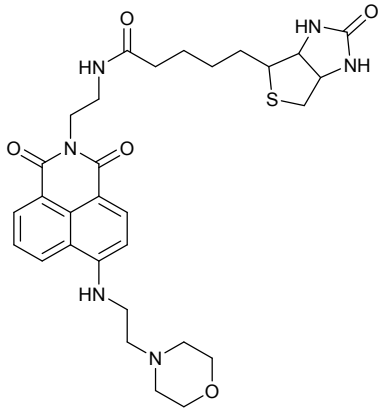
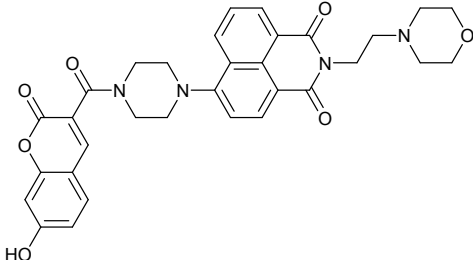
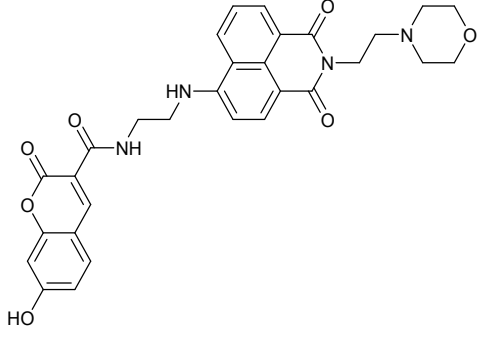
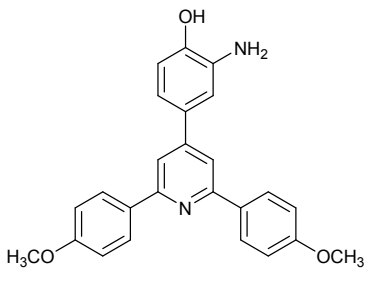
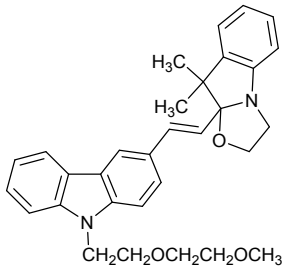
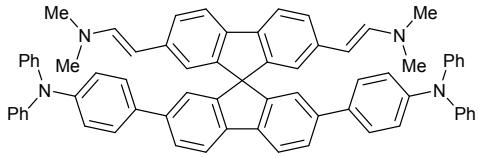
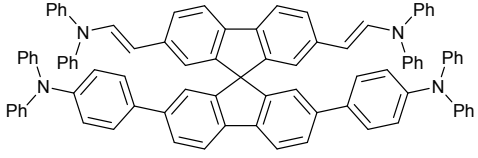
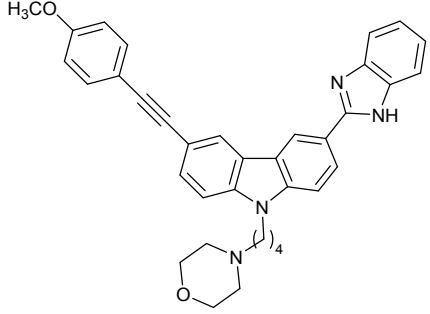
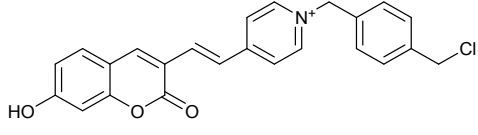


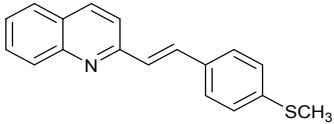
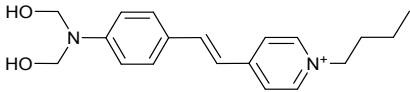
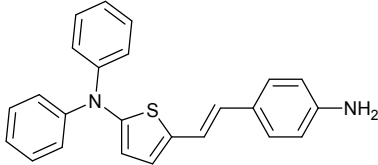
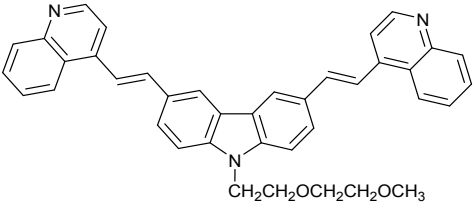
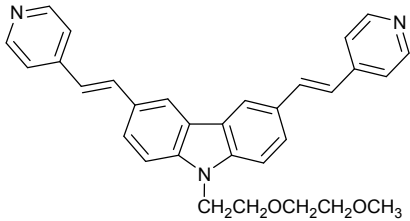
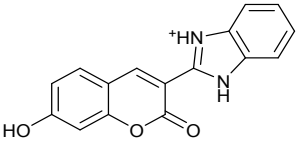
Figure S37: ^1H - ^{13}C -HSQC spectrum of compound **4c** in $\text{DMSO}-d_6$

13. Two-photon pH probes described in literature: benchmark of the state of the art

As yet, most fluorescent pH sensors have been intended to work under single photon excitation. Nevertheless, the additional advantages entailed by two-photon microscopy have aroused the interest of researchers into development of pH probes to be used with this technique. As they are not very numerous, the following table shows the compounds developed for these purpose since 2017 to date. Previous research in this field are summarized in previous reviews.^{9–11}

Compound	λ_{em} (nm)	Cross-section (GM)	pK _a	pH range	Ref.
	460	456 (710 nm)	5.12	4.33–6.73	[12]
	465	411 (700 nm)	3.85	2.99–5.28	[12]
	531	98 (800 nm)	5.36	4.50–5.50	[13]
	555	318 (760 nm)	5.62	4.50–11.00	[14]

	455	---	---	2.00–4.50 6.0–11.00	[14]
	475	--- (700 nm)	3.22	2.40–4.00	[15]
	604	55 (750 nm)	6.60	6.20–7.00	[16]
	486	686 (800 nm)	2.52	1.50–3.50	[17]
	478	914 (800 nm)	2.65	---	[17]
	475	202 (730 nm)	4.86	4.00–5.60	[18]
	550	--- (810 nm)	---	5.00–9.00	[19]

	470	624 (640 nm)	3.21	---	[20]
	590	201 (900 nm)	4.82	3.75–6.00	[21]
	475	42 (800 nm)	---	6.00–8.00	[22]
	550	78 (750 nm)	5.26	5.00–6.00	[23]
	550	110 (750 nm)	4.62	4.30–5.30	[23]
	480	11 (800 nm)	4.20 7.20	3.30–5.40 6.50–8.30	[24]

14. References.

- (1) Benitez-Martin, C.; Guadix, J. A.; Pearson, J. R.; Najera, F.; Perez-Pomares, J. M.; Perez-Inestrosa, E. A Turn-on Two-Photon Fluorescent Probe for Detecting Lysosomal Hydroxyl Radicals in Living Cells. *Sensors Actuators, B Chem.* **2019**, *284*, 744–750. <https://doi.org/10.1016/j.snb.2018.12.163>.
- (2) Brouwer, A. M. Standards for Photoluminescence Quantum Yield Measurements in Solution (IUPAC Technical Report). *Pure Appl. Chem.* **2011**, *83* (12), 2213–2228. <https://doi.org/10.1351/PAC-REP-10-09-31>.
- (3) Terenziani, F.; Katan, C.; Badaeva, E.; Tretiak, S.; Blanchara-Desce, M. Enhanced Two-Photon Absorption of Organic Chromophores: Theoretical and Experimental Assessments. *Adv. Mater.* **2008**, *20* (24), 4641–4678. <https://doi.org/10.1002/adma.200800402>.
- (4) Qiu, L.-Q.; Lai, W. S.; Stumpo, D. J.; Blackshear, P. J. Mouse Embryonic Fibroblast Cell Culture and Stimulation. *Bio-protocol* **2016**, *6* (13). <https://doi.org/10.21769/BioProtoc.1859>.
- (5) Ohkuma, S.; Moriyama, Y.; Takano, T. Identification and Characterization of a Proton Pump on Lysosomes by Fluorescein-Isothiocyanate-Dextran Fluorescence. *Proc. Natl. Acad. Sci. U. S. A.* **1982**, *79* (9), 2758–2762. <https://doi.org/10.1073/pnas.79.9.2758>.
- (6) Frisch, M. J.; Trucks, G. W.; Schlegel, H. B.; Scuseria, G. E.; Robb, M. A.; Cheeseman, J. R.; Scalmani, G.; Barone, V.; Petersson, G. A.; Nakatsuji, H.; et al. Gaussian16 Revision A.03. 2016.
- (7) Tomasi, J.; Mennucci, B.; Cammi, R. Quantum Mechanical Continuum Solvation Models. *Chem. Rev.* **2005**, *105* (8), 2999–3094. <https://doi.org/10.1021/cr9904009>.
- (8) Yanai, T.; Tew, D. P.; Handy, N. C. A New Hybrid Exchange-Correlation Functional Using the Coulomb-Attenuating Method (CAM-B3LYP). *Chem. Phys. Lett.* **2004**, *393* (1–3), 51–57. <https://doi.org/10.1016/j.cplett.2004.06.011>.
- (9) Kim, H. M.; Cho, B. R. Small-Molecule Two-Photon Probes for Bioimaging Applications. *Chem. Rev.* **2015**, *115* (11), 5014–5055. <https://doi.org/10.1021/cr5004425>.
- (10) Lim, C. S.; Cho, B. R. Two-Photon Probes for Biomedical Imaging. *Tetrahedron* **2015**, *71* (43), 8219–8249. <https://doi.org/10.1016/j.tet.2015.06.083>.
- (11) Hou, J.-T.; Ren, W. X.; Li, K.; Seo, J.; Sharma, A.; Yu, X.-Q.; Kim, J. S.; Kikuchi, K.; DeBerardinis, R. J.; Gao, J.; et al. Fluorescent Bioimaging of PH: From Design to Applications. *Chem. Soc. Rev.* **2017**, *46* (8), 2076–2090. <https://doi.org/10.1039/C6CS00719H>.
- (12) Chen, S.; Zhao, M.; Su, J.; Zhang, Q.; Tian, X.; Li, S.; Zhou, H.; Wu, J.; Tian, Y. Two Novel Two-Photon Excited Fluorescent PH Probes Based on the A- π -D- π -A System for Intracellular PH Mapping. *Dye. Pigment.* **2017**, *136*, 807–816. <https://doi.org/10.1016/j.dyepig.2016.09.020>.
- (13) Dong, B.; Song, X.; Kong, X.; Wang, C.; Zhang, N.; Lin, W. A Tumor-Targeting and Lysosome-Specific Two-Photon Fluorescent Probe for Imaging PH Changes in Living Cells. *J. Mater. Chem. B* **2017**, *5* (5), 988–995. <https://doi.org/10.1039/c6tb02957d>.
- (14) Luo, W.; Jiang, H.; Tang, X.; Liu, W. A Reversible Ratiometric Two-Photon Lysosome-Targeted Probe for Real-Time Monitoring of PH Changes in Living Cells. *J. Mater. Chem. B* **2017**, *5* (24), 4768–4773. <https://doi.org/10.1039/c7tb00838d>.
- (15) Ma, J.; Li, W.; Li, J.; Shi, R.; Yin, G.; Wang, R. A Small Molecular PH-Dependent Fluorescent Probe for Cancer Cell Imaging in Living Cell. *Talanta* **2018**, *182*, 464–469. <https://doi.org/10.1016/J.TALANTA.2018.01.088>.
- (16) Xu, D.; Li, Y.; Poon, C. Y.; Chan, H. N.; Li, H. W.; Wong, M. S. A Zero Cross-Talk Ratiometric Two-Photon Probe for Imaging of Acid PH in Living Cells and Tissues and Early Detection of Tumor in Mouse Model. *Anal. Chem.* **2018**, *90* (15), 8800–8806.

<https://doi.org/10.1021/acs.analchem.8b00520>.

- (17) Han, Z.; Tan, J.; Wei, T.; Zhang, Y.; Xiao, H.; Xu, L.; He, B. Two Novel Two-Photon Fluorescent Probes for Low PH Values and Cell Imaging Based on Spirobifluorene Motif. *Sensors Actuators, B Chem.* **2018**, *255*, 2290–2297. <https://doi.org/10.1016/j.snb.2017.09.053>.
- (18) Ning, P.; Hou, L.; Feng, Y.; Xu, G.; Bai, Y.; Yu, H.; Meng, X. Real-Time Visualization of Autophagy by Monitoring the Fluctuation of Lysosomal PH with a Ratiometric Two-Photon Fluorescent Probe. *Chem. Commun.* **2019**, *55* (12), 1782–1785. <https://doi.org/10.1039/C8CC09517E>.
- (19) Jiang, A.; Chen, G.; Xu, J.; Liu, Y.; Zhao, G.; Liu, Z.; Chen, T.; Li, Y.; James, T. D. Ratiometric Two-Photon Fluorescent Probe for: In Situ Imaging of Carboxylesterase (CE)-Mediated Mitochondrial Acidification during Medication. *Chem. Commun.* **2019**, *55* (76), 11358–11361. <https://doi.org/10.1039/c9cc05759e>.
- (20) Dou, Y.; Kenry, K.; Liu, J.; Zhang, F.; Cai, C.; Zhu, Q. 2-Styrylquinoline-Based Two-Photon AIEgens for Dual Monitoring of PH and Viscosity in Living Cells. *J. Mater. Chem. B* **2019**, *7* (48), 7771–7775. <https://doi.org/10.1039/C9TB02036E>.
- (21) Wang, F.; Liu, D.; Shen, Y.; Liu, J.; Li, D.; Tian, X.; Zhang, Q.; Wu, J.; Li, S.; Tian, Y. A Two-Photon Mitochondria-Targeted Fluorescent Probe for the Detection of PH Fluctuation in Tumor and Living Cells. *Dye. Pigment.* **2019**, *166*, 92–97. <https://doi.org/10.1016/j.dyepig.2019.03.033>.
- (22) Lu, X.; Zhang, G.; Li, D.; Tian, X.; Ma, W.; Li, S.; Zhang, Q.; Zhou, H.; Wu, J.; Tian, Y. Thiophene Aromatic Amine Derivatives with Two-Photon Activities as Probes for the Detection of Picric Acid and PH. *Dye. Pigment.* **2019**, *170*, 107641. <https://doi.org/10.1016/j.dyepig.2019.107641>.
- (23) Zhang, T.; Xu, D.; Poon, C. Y.; Wang, X.; Bolze, F.; Li, H. W.; Wong, M. S. Tuning the PKa of Two-Photon Bis-Chromophoric Probes for Ratiometric Fluorescence Imaging of Acidic PH in Lysosomes. *Talanta* **2019**, *202*, 34–41. <https://doi.org/10.1016/j.talanta.2019.04.042>.
- (24) Jiang, X.; Liu, Z.; Yang, Y.; Li, H.; Qi, X.; Ren, W. X.; Deng, M.; Lü, M.; Wu, J.; Liang, S. A Mitochondria-Targeted Two-Photon Fluorescent Probe for Sensing and Imaging PH Changes in Living Cells. *Spectrochim. Acta - Part A Mol. Biomol. Spectrosc.* **2020**, *224*, 117435. <https://doi.org/10.1016/j.saa.2019.117435>.